On the stability and transition of Marangoni convection of two immiscible fluids with a non-deformable interface

Chao Xing^a, Daozhi Han^b, Quan Wang^{c,*}

Abstract

This article investigates the nonlinear stability and dynamic transition involving the Marangoni convection of two superimposed immiscible fluids subject to temperature gradient perpendicular to the plate. First, we obtain the critical value of the Marangoni number and verify the stability exchange principle by adopting a hybrid method that combines theoretical analysis and numerical calculations. Second, we use energy method to discuss the nonlinear stability and to establish the nonlinear thresholds of the Marangoni number. Third, we apply the technique of center manifold reduction to reduce the corresponding infinite dimensional model to a finite dimensional ordinary differential equations. According to the ordinary differential equations, we establish nonlinear transition theorem with a non-dimensional coefficient that determines the transition type of the model. Finally, we determine the non-dimensional coefficient and present related temporal and flow patterns by numerical computation. The existence and uniqueness of global weak solution to the model is also given in the appendix.

Keywords: Bifurcation, Dynamic transition, Center manifold, Two-fluid, Marangoni-Bénard convection, Non-deformable interface.

^a College of Applied Mathematics, Chengdu University of Information Technology, Chengdu, 610225, P. R. China

b Department of Mathematics, The State University of New York at Buffalo, Buffalo, NY 14260 USA

^cDepartment of Mathematics, Sichuan University, Chengdu, 610064, P. R. China

^{*}Corresponding author

Email addresses: xingchao@cuit.edu.cn (Chao Xing), Daozhiha@buffalo.edu (Daozhi Han), wangquan@indiana.edu (Quan Wang)

1. Introduction

Interfacial convection is a striking phenomenon that takes place any time the interfacial tension is not uniform along the interface between two fluids. This type of convection is a basic mechanism of fluid motion under microgravity conditions [1, 2]. Interfacial convection is also crucial in microfluidic systems, where it provides a mechanism for mixing [3, 4] and a reliable transport mechanism [5, 6, 7]. Interfacial convection not only plays an important role in modern engineering processes, such as mentioning laser welding [8, 9], ordering of nanoparticles [10, 11] and fabrication of microporous polymer film [12, 13, 14, 15], but also are significant for various biological processes [16, 17] and materials processing [18]. These numerous applications of the interfacial convection cause a need for physical and mathematical study.

The thermocapillary effect is the dependence of the surface tension on the temperature, which is the normal physical effect that produce Interfacial convection in fluids [19]. Typically, the surface tension decreases when the temperature grows. This type of convection is called Marangoni convection, which have been intensively studied by both applied mathematicians and physicists [20, 21, 22, 23, 24, 25, 26, 27, 28] with linear and nonlinear analysis.

In reality, an interface between a liquid and a gas is a simplified as the free surface, leading that one-layer model is generally applied to study the Marangoni convection. Then, the full problem for the fluid motion and for the heat/mass transfer involving Marangoni convection is formulated only in the liquid phase, whereas the influence of the gas phase is described in a phenomenological way by means of the Biot number. For detailed study involving Marangoni convection with one-layer model, we refer readers to [29, 30, 31, 28, 32] and many other.

The one-layer approach is not sufficient for the description of many phenomena caused by processes in fluids on both sides of the interface. These phenomena can not be understood without an analysis of the interfacial hy-

drodynamic and thermal interaction between both fluids. For example, for the onset of Marangoni convection in a liquid-gas system, the one-layer approach predicts the monotonic Marangoni instability only for heating from the side of the liquid [33]. The two-layer approach reveals the appearance of the monotonic Marangoni instability for both ways of heating, depending on the ratio of layers thicknesses [34]. In addition, it is well-known that the stability problem for the mechanical equilibrium state in a system with an interface is not self-adjoint [35], which means that the one-layer approach is unable to reveal several oscillatory instabilities in systems with a non-deformable interface [36].

Due to the applications of two-layer Marangoni convection in engineering technology, chemical engineering, mechanical metallurgical engineering, microelectronics industry, this type of convection has been extensively studied from different angles. Engel and Swift [37] investigated the convection pattern of two layer Marangoni convection with non-deformable interface by using weakly non-linear analysis. Mo and Ruan [38, 39] studied the linear stability analysis of thermocapillary convection in an annular two layer system to radial temperature. Madruga et al [40] discussed the linear stability problem of a two-layer fluid with a non-deformable interface subject to horizontal temperature gradient. Simanovskii and Kabov [41] utilized numerical methods to study the oscillating convection with non-deformable interface. Tavener and Cliffe [42] described numerical method of two-layer Marangoni convectoin with deformable interface and linear stability of the model. Lyubimova and Parshakova [43] investigated the long wave instability of two layer system with deformable interface. For more works on two-layer Marangoni convection problems with non-deformable and deformable interface, we refer readers to [44, 45, 46, 47, 48, 49]

In the paper, our main goal is to study Marangoni convection problem of of two superimposed immiscible fluids by using a two-layer model from the perspective of nonlinear stability and dynamic transition. The model is bounded in the vertical direction and is infinite in the horizontal direction. The interface between two fluid layers is assumed to be non-deformable, because short-wave Marangoni instability is insensitive to the interface deformation, as pointed in [19]. The mathematical tool that we use is the dynamic transition theory [50] established to understand phase transition phenomena in nonlinear dissipative systems. The primary idea of dynamic transition theory is to find a complete set of transition states and give a complete description of instabilities and the corresponding nonlinear dynamic transitions. The dynamic transition theory has been used extensively to study phase transition phenomena in fluid sciences [51, 28, 52, 53, 54]. Dijkstra, Sengul, et al [28] discussed dynamic transition types of single layer fluid Marangoni convection system. Very recently, Han et al [52] investigated dynamic transition for the Rayleigh-Bénard convection in the superposed free flow and porous media. Additionally, to our knowledge, there is little literature on the dynamic transitions of Marangoni convection of two superimposed immiscible fluids. Physically, it is vey important to know how the height ratio, density ratio and other parameters of the fluid layer affect the phase transition type of Marangoni convection of he two-layer fluids.

Let us briefly describe the main conclusions of this article. First, we obtain the critical values of Marangoni number, verifies that PES condition and establish nonlinear transition theorem. For the special case where the thickness of the upper fluid is equal to the thickness of the lower fluid, the explicit expression of the critical values is derived. For generic cases, we use the Chebyshev tau method to estimate the critical values, and discuss the influence of height ratio, aspect ratio, density ratio, and heat capacity ratio on them. Second, we reduce the infinite dimensional model to a complex-valued ordinary differential equations by utilizing the method of center manifold reduction. With the help of the reduced equations, we deduce a transition theorem along with a dimensionless coefficient Q used for determination of transition types. Finally, Our numerical results show that both jump and continuous transition occur in two superimposed immiscible fluids, which is different from single layer fluid Marangoni-Bénard convection [28]. In the appendix, we give the existence and uniqueness of global weak solution by using the Galerkin method.

The rest of this paper is organized as follows. In section 2, we present the Boussinesq model which describes two superimposed immiscible fluids and rewrite the model as an abstract equation. In section 3, we study the linear eigenvalue and verify PES. In section 4, we analyze nonlinear stability. In section 5, based on the PES and reduction on center manifold, the dynamic transition theorem is given. In section 6, some numerical results are given to illustrate the theoretical results. In section 7, the conclusions are summarized. In section appendix, we discuss the existence and uniqueness of weak solution.

2. Governing Equations

2.1. Nondimensionalization

We consider Marangoni convection involving two immiscible fluids in finite two-dimensional domains $\Omega = \Omega_1 \cup \Omega_2$ sketched in Figure 2.1, where Ω_1 and Ω_2 satisfy that $\bar{\Omega}_1 \cap \bar{\Omega}_2 = \Gamma_i$ which represents the interface between two immiscible fluids. Because short-wave Marangoni instability is insensitive to the interface deformation, as pointed in [19], we can disregard the interface deformations. We then assume that the interface Σ is flat and lies in x axis.

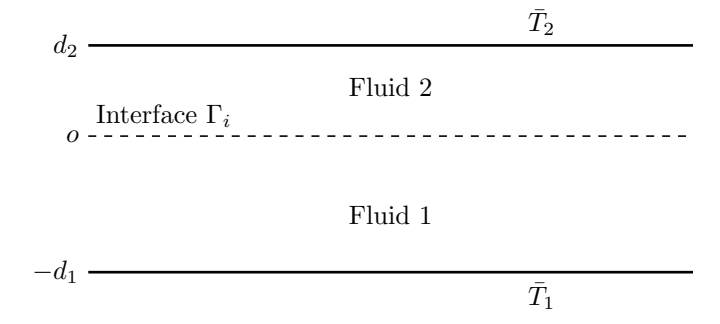


Figure 2.1: Sketch of the physical domain. Ω_1 : the lower fluid region. Ω_2 : the upper fluid region. Γ_i denotes the interface

The nonlinear equations of convection in the framework of the Boussinesq approximation have the following form

$$\operatorname{div}\mathbf{u_m} = 0, \tag{2.1}$$

$$\bar{\rho}_m(\frac{\partial \mathbf{u}_m}{\partial t} + (\mathbf{u}_m \cdot \nabla)\mathbf{u}_m) = -\nabla p_m + \mu_m \nabla^2 u_m - g\bar{\rho}_m \mathbf{j}[1 - \alpha_m (T_m - \bar{T})], (2.2)$$

$$\bar{\rho}_m c_m \left(\frac{\partial T_m}{\partial t} + (\mathbf{u}_m \cdot \nabla) T_m \right) = k_m \nabla^2 T_m, \tag{2.3}$$

where the subscript m=1,2 denotes the lower and upper fluids, respectively, the unknown function $\mathbf{u}_m=(u_m,v_m)$ is the velocity, T_m is the temperature, p_m is the pressure, $\bar{\rho}_m$ denotes the density of liquid m, \bar{T} is a fixed reference temperature, α_m is the thermal expansion coefficients, k_m is the thermal conductivity, c_m is the specific heat capacity, and μ_m is the molecular diffusivity.

The boundary conditions at flat interface y = 0 are well-known, they are

$$v_1 = v_2 = 0, \ u_1 = u_2, \ T_1 = T_2,$$
 (2.4)

$$\mu_2 \frac{\partial u_2}{\partial y} - \mu_1 \frac{\partial u_1}{\partial y} + \delta_1 \frac{\partial T_1}{\partial x} = 0, \tag{2.5}$$

$$k_2 \frac{\partial T_2}{\partial y} - k_1 \frac{\partial T_1}{\partial y} = 0, \tag{2.6}$$

where the interfacial tension at the interface has been assumed to be a linear function $\delta = \delta_0 - \delta_1(T_1 - T_0)$. The first condition at interface means the continuity of the velocity field and the temperature field, the second condition at interface represents the balance of tangential stresses, and the third condition at interface means the continuity of the heat flux normal components.

We also utilize the following boundary conditions at the rigid boundaries

$$\frac{\partial u_1}{\partial y} = v_1 = 0, \ T_1 = \bar{T}_1, \text{ at } y = -d_1,$$
 (2.7)

$$\frac{\partial u_2}{\partial y} = v_2 = 0, \ T_2 = \bar{T}_2, \ \text{at } y = d_2,$$
 (2.8)

with $\bar{T}_1 - T_0 > 0$ for heating from below.

From the system of equations (2.1)-(2.8), it has the basic solution given by

$$\mathbf{u}_{1b} = \mathbf{u}_{2b} = \mathbf{0}, \ T_{1b} = -\frac{\bar{T}_1 - T_0}{d_1}y + T_0, \ T_{2b} = -\frac{T_0 - \bar{T}_2}{d_2}y + T_0, \tag{2.9}$$

where $T_0 = \frac{\bar{T}_1 k_1 d_2 + \bar{T}_2 k_2 d_2}{k_1 d_2 + k_2 d_1}$, and the pressures satisfy the following equations

$$\nabla p_{mb} = -g\bar{\rho}_{m}\mathbf{j}[1 - \alpha_{m}(T_{mb} - \bar{T})], \ (m = 1, 2).$$

To consider the stability of the above steady-state solution, we make the following transformations

$$\mathbf{u}'_{m} = \mathbf{u}_{m}, \ T'_{m} = T_{m} - T_{mb}, \ p'_{m} = p_{m} - p_{mb},$$
 (2.10)

as well as

$$x = d\tilde{x}, \ y = d\tilde{y}, \ \kappa_1 = \frac{k_1}{\bar{\rho}_1 c_1}, t = \frac{d^2}{\kappa_1} \tilde{t}, \ p'_m = \frac{\mu_1 \kappa_1}{d^2} \tilde{p}_m,$$
$$\mathbf{u}'_m = \frac{\kappa_1}{d} \tilde{\mathbf{u}}_m, \ T'_m = (\bar{T}_1 - T_0) \tilde{T}_m, \ m = 1, 2.$$
(2.11)

Substituting (2.10) and (2.11) into (2.1)-(2.3), omitting the tilde and ignoring the effects of gravity, we derive the non-dimensional perturbation equations

$$\frac{\partial \mathbf{u}_1}{\partial t} + (\mathbf{u}_1 \cdot \nabla)\mathbf{u}_1 = -Pr\nabla p_1 + Pr\nabla^2 \mathbf{u}_1, \tag{2.12}$$

$$\frac{\partial T_1}{\partial t} + (\mathbf{u}_1 \cdot \nabla)T_1 = \nabla^2 T_1 + \frac{1}{\tilde{d}_1} v_1, \tag{2.13}$$

$$\operatorname{div}\mathbf{u}_1 = 0, \tag{2.14}$$

and

$$\frac{\partial \mathbf{u}_2}{\partial t} + (\mathbf{u}_2 \cdot \nabla)\mathbf{u}_2 = -\frac{Pr}{\rho_r} \nabla p_2 + \frac{Pr}{\rho_r} \mu_r \nabla^2 \mathbf{u}_2, \tag{2.15}$$

$$\frac{\partial T_2}{\partial t} + (\mathbf{u}_2 \cdot \nabla)T_2 = \frac{k_r}{\rho_r c_r} \nabla^2 T_2 + \frac{1}{k_r} \frac{1}{\tilde{d}_1} v_2, \tag{2.16}$$

$$\operatorname{div}\mathbf{u}_2 = 0. \tag{2.17}$$

Substituting (2.10) and (2.11) into (2.4)-(2.8), we derive that the boundary condition at the interface y = 0 are

$$v_1 = v_2 = 0, \ u_1 = u_2, \ T_1 = T_2,$$
 (2.18)

$$\mu_r \frac{\partial u_2}{\partial y} - \frac{\partial u_1}{\partial y} + Ma \frac{\partial T_1}{\partial x} = 0, \qquad (2.19)$$

$$k_r \frac{\partial T_2}{\partial y} - \frac{\partial T_1}{\partial y} = 0. {(2.20)}$$

And, the boundary condition (2.7)-(2.8) are rewritten as

$$\frac{\partial u_1}{\partial y} = v_1 = T_1 = 0, \ y = -\tilde{d}_1,$$
 (2.21)

$$\frac{\partial u_2}{\partial y} = v_2 = T_2 = 0, \ y = \tilde{d}_2.$$
 (2.22)

It is natural to assume that perturbations are periodic in x-direction, i.e.

$$\mathbf{u}_m(0,y) = \mathbf{u}_m(\tilde{l},y), \ T_m(0,y) = T_m(\tilde{l},y), \ m = 1,2.$$
 (2.23)

where \tilde{l} is the spatial period. For these nondimensional parameters appearing in the equations (2.15)-(2.17)., let us give their explicit expressions. The Prandtl number (Pr) and Marangoni number (Ma) are defined as follows

$$Pr = \frac{\nu_1}{\kappa_1}, \ \nu_1 = \frac{\mu_1}{\bar{\rho}_1}, \ Ma = \frac{\delta_1 d(\bar{T}_1 - T_0)}{\mu_1 \kappa_1}.$$

Moreover, the ratios appearing in the equations (2.15)-(2.17) are

$$\rho_r = \frac{\bar{\rho}_2}{\bar{\rho}_1}, \quad \mu_r = \frac{\mu_2}{\mu_1}, \quad c_r = \frac{c_2}{c_1}, \quad k_r = \frac{k_2}{k_1}, \quad \tilde{l} = \frac{l}{d}, \quad \tilde{d}_1 = \frac{d_1}{d}, \quad \tilde{d}_2 = \frac{d_2}{d}.$$

For initial data for the equations (2.15)-(2.17), let us set

$$\mathbf{u}_1(0,x) = \mathbf{u}_{10}, \ T_1(0,x) = T_{10}, \ \mathbf{u}_2(0,x) = \mathbf{u}_{20}, \ T_2(0,x) = T_{20}.$$
 (2.24)

2.2. Abstract Form

In this subsection, we shall rewrite (2.12)-(2.24) as an abstract form. First, let us introduce some relevant function spaces as follows

$$V = \{ \psi = (\mathbf{u_1}, T_1, \mathbf{u_2}, T_2) \in [H^1(\Omega_1)]^3 \times [H^1(\Omega_2)]^3 : \text{div}\mathbf{u_1} = 0, \text{div}\mathbf{u_2} = 0,$$

and ψ satisfies $(2.18) - (2.22)\},$

$$H = \{ \psi = (\mathbf{u_1}, T_1, \mathbf{u_2}, T_2) \in [L^2(\Omega_1)]^3 \times [L^2(\Omega_2)]^3 : \operatorname{div} \mathbf{u_1} = 0, \operatorname{div} \mathbf{u_2} = 0, \mathbf{u_1} \cdot \mathbf{n_1} = 0, \mathbf{u_2} \cdot \mathbf{n_2} = 0 \},$$

which are equipped with the following norms, respectively,

$$\begin{aligned} ||\psi||_{V} &= [||\mathbf{u_{1}}||_{(H^{1}(\Omega_{1}))^{2}}^{2} + ||T_{1}||_{H^{1}(\Omega_{1})}^{2} + ||\mathbf{u_{2}}||_{(H^{1}(\Omega_{2}))^{2}}^{2} + ||T_{2}||_{H^{1}(\Omega_{2})}^{2}]^{\frac{1}{2}}, \\ ||\psi||_{H} &= [||\mathbf{u_{1}}||_{(L^{2}(\Omega_{1}))^{2}}^{2} + ||T_{1}||_{L^{2}(\Omega_{1})}^{2} + ||\mathbf{u_{2}}||_{(L^{2}(\Omega_{2}))^{2}}^{2} + ||T_{2}||_{L^{2}(\Omega_{2})}^{2}]^{\frac{1}{2}}. \end{aligned}$$

It is not hard to see that V and H are separable Hilbert spaces. We denote the inner product on Hilbert spaces H and V by $(.,.)_V = (.,.)_{H^1(\Omega_1)} + (.,.)_{H^1(\Omega_2)}$ and $(,..)_V = (.,.)_{L^2(\Omega_1)} + (.,.)_{L^2(\Omega_2)}$, respectively.

For convenience, let us use $(, .,)_i$ to denote the inner product on the spaces $L^2(\Omega_i)(i=1,2)$. For $\psi=(\mathbf{u_1},T_1,\mathbf{u_2},T_2)\in V$, due to

$$(\nabla p_i, \mathbf{u}_i)_i = 0, \ i = 1, 2, \tag{2.25}$$

by (2.25), we then define the linear operator $L_{Ma}: V \to H$ as follows

$$(L_{Ma}\psi,\tilde{\psi})$$

$$= -Pr(\nabla \mathbf{u_1}, \nabla \tilde{\mathbf{u}}_1)_1 - (\nabla T_1, \nabla \tilde{T}_1)_1 + \frac{1}{\tilde{d}_1} (v_1, \tilde{T}_1)_1 - \frac{Pr\mu_r}{\rho_r} (\nabla \mathbf{u_2}, \nabla \tilde{\mathbf{u}}_2)_2$$

$$- \frac{k_r}{\rho_r c_r} (\nabla T_2, \nabla \tilde{T}_2)_2 + \frac{1}{\tilde{d}_1} \frac{1}{k_r} (v_2, \tilde{T}_2)_2 + Pr \int_{y=0} \frac{\partial u_1}{\partial y} \tilde{u}_1 ds + \int_{y=0} \frac{\partial T_1}{\partial y} \tilde{T}_1 ds$$

$$- \frac{Pr\mu_r}{\rho_r} \int_{y=0} \frac{\partial u_2}{\partial y} \tilde{u}_2 ds - \frac{k_r}{\rho_r c_r} \int_{y=0} \frac{\partial T_2}{\partial y} \tilde{T}_2 ds, \qquad (2.26)$$

where $\tilde{\psi} = (\tilde{\mathbf{u}}_1, \tilde{T}_1, \tilde{\mathbf{u}}_2, \tilde{T}_2) \in V$. We also define operator $G: V \to H$ by

$$(G(\psi, \psi), \tilde{\psi}) = ((\mathbf{u}_1 \cdot \nabla)\mathbf{u}_1, \tilde{\mathbf{u}}_1)_1 + ((\mathbf{u}_1 \cdot \nabla)T_1, \tilde{T}_1)_1 + ((\mathbf{u}_2 \cdot \nabla)\mathbf{u}_2, \tilde{\mathbf{u}}_2)_2$$

$$+ ((\mathbf{u}_1 \cdot \nabla)T_2, \tilde{T}_2)_2.$$

$$(2.27)$$

For simplicity, we will use the abbreviation $G(\psi) := G(\psi, \psi)$. Therefore, combining (2.26)-(2.27), the problem (2.12)-(2.24) can be rewritten as

$$\begin{cases} \frac{d\psi}{dt} = L_{Ma}\psi + G(\psi), \\ \psi(0) = \psi_0, \end{cases}$$
 (2.28)

where $\psi_0 = (\mathbf{u}_{10}, T_{10}, \mathbf{u}_{20}, T_{20})$ is the initial condition.

3. Linear stability and principle of exchange of stabilities

3.1. Principle of exchange of stabilities

It is well known that the stability of the zero solutions to the system of equations (2.12)-(2.24) are determined by the signs of eigenvalues of the corresponding linear operator. The eigenvalue problem of (2.12)-(2.24) read

$$Pr(-\frac{\partial p_1}{\partial x} + \nabla^2 u_1) = \beta u_1,$$

$$Pr(-\frac{\partial p_1}{\partial y} + \nabla^2 v_1) = \beta v_1, \ (x, y) \in (0, \tilde{l}) \times (-\tilde{d}_1, 0),$$

$$\nabla^2 T_1 + \frac{1}{\tilde{d}_1} v_1 = \beta T_1,$$

$$\frac{\partial u_1}{\partial x} + \frac{\partial v_1}{\partial y} = 0,$$
(3.1)

and

$$\frac{Pr}{\rho_r} \left(-\frac{\partial p_2}{\partial x} + \mu_r \nabla^2 u_2 \right) = \beta u_2,
\frac{Pr}{\rho_r} \left(-\frac{\partial p_2}{\partial y} + \mu_r \nabla^2 v_2 \right) = \beta v_2, \quad (x, y) \in (0, \tilde{l}) \times (0, \tilde{d}_2),
\frac{k_r}{\rho_r c_r} \nabla^2 T_2 + \frac{1}{\tilde{d}_1} \frac{1}{k_r} v_2 = \beta T_2,
\frac{\partial u_2}{\partial x} + \frac{\partial v_2}{\partial y} = 0.$$
(3.2)

Utilizing (2.25), the interface condition (2.18)-(2.20) and boundary condition (2.23)-(2.22), the weak form of the preceding eigenvalue problem can be given

$$\beta(\mathbf{u}_{1}, \tilde{\mathbf{u}}_{1})_{1} + \beta(T_{1}, \tilde{T}_{1})_{1} + \beta\rho_{r}(\mathbf{u}_{2}, \tilde{\mathbf{u}}_{2})_{2} + \rho_{r}c_{r}\beta(T_{2}, \tilde{T}_{2})_{2}$$

$$= -Pr(\nabla \mathbf{u}_{1}, \nabla \tilde{\mathbf{u}}_{1})_{1} - (\nabla T_{1}, \nabla \tilde{T}_{1})_{1} - \mu_{r}Pr(\nabla \mathbf{u}_{2}, \nabla \tilde{\mathbf{u}}_{2})_{2} - k_{r}(\nabla T_{2}, \nabla \tilde{T}_{2})_{2}$$

$$+ \frac{1}{\tilde{d}_{1}}(v_{1}, \tilde{T}_{1})_{1} + \rho_{r}c_{r}\frac{1}{\tilde{d}_{1}}\frac{1}{k_{r}}(v_{2}, \tilde{T}_{2})_{2} + PrMa\int_{y=0}^{z} \frac{\partial T_{1}}{\partial x}\tilde{u}_{1}ds. \tag{3.3}$$

In fact, the equation (3.3) has an abstract form. Let us define the bilinear operators \mathcal{A} and \mathcal{B} on $V \times V$ as follows

$$\mathcal{A}(\psi, \widetilde{\psi}) = -Pr(\nabla \mathbf{u}_1, \nabla \widetilde{\mathbf{u}}_1)_1 - (\nabla T_1, \nabla \widetilde{T}_1)_1 - Pr\mu_r(\nabla \mathbf{u}_2, \nabla \widetilde{\mathbf{u}}_2)_2$$
$$-k_r(\nabla T_2, \nabla \widetilde{T}_2)_2, \tag{3.4}$$

$$\mathcal{B}_{Ma}(\psi, \widetilde{\psi}) = \frac{1}{\tilde{d}_1} (v_1, \tilde{T}_1)_1 + \rho_r c_r \frac{1}{\tilde{d}_1} \frac{1}{k_r} (v_2, \tilde{T}_2)_2 + PrMa \int_{y=0}^{z} \frac{\partial T_1}{\partial x} \tilde{u}_1 ds. \quad (3.5)_{y=0}^{z} \tilde{u}_1 ds.$$

Riesz represent theorem implies that there exist operators $A, B_{Ma}: V \to V^*$ such that $\mathcal{A}(\psi, \widetilde{\psi}) = \langle A\psi, \widetilde{\psi} \rangle$, $\mathcal{B}_{Ma}(\psi, \widetilde{\psi}) = \langle B_{\lambda}\psi, \widetilde{\psi} \rangle$. We then define $L_{Ma}\psi = A\psi + B_{Ma}\psi$. Hence, the abstract form of the equation (3.3) can be given by

$$L_{Ma}\psi = \beta M\psi, \tag{3.6}$$

where M is a matrix given by

$$M = egin{pmatrix} 1 & 0 & 0 & 0 & 0 & 0 & 0 \ 0 & 1 & 0 & 0 & 0 & 0 \ 0 & 0 & 1 & 0 & 0 & 0 & 0 \ 0 & 0 & 0 &
ho_r & 0 & 0 & 0 \ 0 & 0 & 0 & 0 &
ho_r & 0 & 0 \ 0 & 0 & 0 & 0 & 0 & c_r
ho_r \end{pmatrix}.$$

Apparently, there exist countably infinitely many discrete eigenvalues to the eigenvalue problem (3.6), which can be ordered as

$$\operatorname{Re}\beta_1(Ma) \ge \operatorname{Re}\beta_2(Ma) \ge \dots \to -\infty.$$
 (3.7)

Additionally, using the following definition of the dual operator L_{Ma}

$$(L_{Ma}\psi, \psi^*) = (\psi, L_{Ma}^*\psi^*),$$
 (3.8)

the eigenvalue problem associated with the dual operator L_{Ma}^* is given by

$$Pr(-\frac{\partial p_1^*}{\partial x} + \nabla^2 u_1^*) = \overline{\beta} u_1^*,$$

$$Pr(-\frac{\partial p_1^*}{\partial y} + \nabla^2 v_1^*) + \frac{1}{\tilde{d}_1} T_1^* = \overline{\beta} v_1^*, \ (x, y) \in (0, \tilde{l}) \times (-\tilde{d}_1, 0),$$

$$\nabla^2 T_1^* = \overline{\beta} T_1^*,$$

$$\frac{\partial u_1^*}{\partial x} + \frac{\partial v_1^*}{\partial y} = 0,$$
(3.9)

and

$$\frac{Pr}{\rho_r} \left(-\frac{\partial p_2^*}{\partial x} + \mu_r \nabla^2 u_2^* \right) = \overline{\beta} u_2^*,
\frac{Pr}{\rho_r} \left(-\frac{\partial p_2^*}{\partial y} + \mu_r \nabla^2 v_2^* \right) + \frac{1}{\tilde{d}_1} \frac{1}{k_r} T_2^* = \overline{\beta} v_2^*, \quad (x, y) \in (0, \tilde{l}) \times (0, \tilde{d}_2),
\frac{k_r}{\rho_r c_r} \nabla^2 T_2^* = \overline{\beta} T_2^*,$$
(3.10)

$$\frac{\partial u_2^*}{\partial x} + \frac{\partial v_2^*}{\partial y} = 0,$$

which subject to the same boundary conditions (2.23)-(2.22), but the interface condition is different, which is given by

$$v_1^* = v_2^* = 0, \ \rho_r u_1^* = u_2^*, \ \rho_r c_r T_1^* = T_2^*,$$
 (3.11)

$$\frac{\mu_r}{\rho_r} \frac{\partial u_2^*}{\partial y} = \frac{\partial u_1^*}{\partial y},\tag{3.12}$$

$$\frac{k_r}{\rho_r c_r} \frac{\partial T_2^*}{\partial y} - \frac{\partial T_1^*}{\partial y} + PrMa \frac{\partial v_1^*}{\partial y} = 0. \tag{3.13}$$

Denote $\gamma_1 = \frac{2m\pi}{l}$ and $D = \frac{d}{dy}$. Using the method of separation of variables, we look for the solutions to the equations (3.1)-(3.2) in the following forms:

$$u_j = \phi_j(y) \exp(i\gamma_1 x), \quad v_j = \varphi_j(y) \exp(i\gamma_1 x),$$
 (3.14)

$$T_i = \theta_i(y) \exp(i\gamma_1 x), \ p_i = \eta_i(y) \exp(i\gamma_1 x), j = 1, 2.$$
 (3.15)

substituting (3.14)-(3.15) into (3.1)-(3.2) and eliminating p_j , we have

$$Pr(D^{2} - \gamma_{1}^{2})^{2}\varphi_{1} = \beta(D^{2} - \gamma_{1}^{2})\varphi_{1}, \tag{3.16}$$

$$(D^{2} - \gamma_{1}^{2})\theta_{1} + \frac{1}{\tilde{d}_{1}}\varphi_{1} = \beta\theta_{1}, \quad y \in (-\tilde{d}_{1}, 0), \tag{3.17}$$

and

$$\mu_r Pr \rho_r^{-1} (D^2 - \gamma_1^2)^2 \varphi_2 = \beta (D^2 - \gamma_1^2) \varphi_2, \tag{3.18}$$

$$k_r \rho_r^{-1} c_r^{-1} (D^2 - \gamma_1^2) \theta_2 + \frac{1}{\tilde{d}_1} \frac{1}{k_r} \varphi_2 = \beta \theta_2, \quad y \in (0, \tilde{d}_2).$$
 (3.19)

By the interface conditions (2.18)-(2.20) and the boundary conditions (2.23)-(2.22), we have

$$\varphi_1(0) = \varphi_2(0) = 0, \ D\varphi_1(0) = D\varphi_2(0), \ \theta_1(0) = \theta_2(0),$$
 (3.20)

$$\mu_T D^2 \varphi_2(0) - D^2 \varphi_1(0) + \gamma_1^2 M a \theta_1(0) = 0, \tag{3.21}$$

$$k_r D\theta_2(0) - D\theta_1(0) = 0, (3.22)$$

$$D^{2}\varphi_{1}(-\tilde{d}_{1}) = \varphi_{1}(-\tilde{d}_{1}) = \theta_{1}(-\tilde{d}_{1}) = 0, \tag{3.23}$$

$$D^{2}\varphi_{2}(\tilde{d}_{2}) = \varphi_{2}(\tilde{d}_{2}) = \theta_{2}(\tilde{d}_{2}) = 0. \tag{3.24}$$

Similarly, we obtain the equations to the adjoint problem

$$Pr(D^{2} - \gamma_{1}^{2})^{2} \varphi_{1}^{*} - \gamma_{1}^{2} \frac{1}{\tilde{d}_{1}} \theta_{1}^{*} = \bar{\beta}(D^{2} - \gamma_{1}^{2}) \varphi_{1}^{*}, \tag{3.25}$$

$$(D^2 - \gamma_1^2)\theta_1^* = \bar{\beta}\theta_1^*, \tag{3.26}$$

and

$$Pr\mu_r \rho_r^{-1} (D^2 - \gamma_1^2)^2 \varphi_2^* - \gamma_1^2 \frac{1}{k_r \tilde{d}_1} \theta_2^* = \bar{\beta} (D^2 - \gamma_1^2) \varphi_2^*, \tag{3.27}$$

$$kr\rho_r^{-1}c_r^{-1}(D^2 - \gamma_1^2)\theta_2^* = \bar{\beta}\theta_2^*,$$
 (3.28)

with the following boundary condition and interface condition

$$\begin{split} \varphi_1^*(0) &= \varphi_2^*(0) = 0, \; \rho_r D \varphi_1^*(0) = D \varphi_2^*(0), \\ \rho_r c_r \theta_1^*(0) &= \theta_2^*(0), \; D^2 \varphi_1^*(0) = \frac{\mu_r}{\rho_r} D^2 \varphi_2^*(0), \\ \frac{k_r}{\rho_r c_r} D \theta_2^*(0) - D \theta_1^*(0) + Pr Ma D \varphi_1^*(0) = 0, \\ D^2 \varphi_1^*(-\tilde{d}_1) &= \varphi_1^*(-\tilde{d}_1) = \theta_1^*(-\tilde{d}_1) = 0, \\ D^2 \varphi_2^*(\tilde{d}_2) &= \varphi_2^*(\tilde{d}_2) = \theta_2^*(\tilde{d}_2) = 0. \end{split}$$

Assuming that the first eigenvalue $\beta_1(Ma) \in R$. For the special case $\tilde{d}_1 = \tilde{d}_2$, we obtain the critical value Ma_c of Marangoni number Ma by solving the problem (3.16)-(3.24) with $\beta = 0$, which is

$$Ma_{c} = \min_{\gamma_{1} > 0} \frac{2(1 + \mu_{r})\sinh^{2}(\gamma_{1}\tilde{d}_{1})}{\gamma_{1} \left[\tilde{C}_{11}\sinh(\gamma_{1}\tilde{d}_{1}) + \psi_{11}(0)\sinh(\gamma_{1}\tilde{d}_{1}) + \psi_{12}(0)\cosh(\gamma_{1}\tilde{d}_{1})\right]},$$
(3.29)

where

$$\begin{split} \tilde{C}_{11} &= \frac{2(h_1 k_r \cosh(\gamma_1 \tilde{d}_1) + h_2 \sinh(\gamma_1 \tilde{d}_1))}{(1 + k_r) \sinh(2\gamma_1 \tilde{d}_1)}, \\ h_1 &= -\psi_{11}(0) \sinh(\gamma_1 \tilde{d}_1) - \psi_{12}(0) \cosh(\gamma_1 \tilde{d}_1) - \psi_{22}(\tilde{d}_1) \cosh(\gamma_1 \tilde{d}_1), \\ h_2 &= k_r \psi_{22}(\tilde{d}_1) \sinh(\gamma_1 \tilde{d}_1) - \psi_{11}(0) \cosh(\gamma_1 \tilde{d}_1) - \psi_{12}(0) \sinh(\gamma_1 \tilde{d}_1), \end{split}$$

and

$$\psi_{11}(0) = -\frac{1}{\gamma_1 \tilde{d}_1} \left\{ \frac{1}{4\gamma_1} \sinh(\gamma_1 \tilde{d}_1) \tilde{d}_1 \sinh(2\gamma_1 \tilde{d}_1) + (1 - \cosh(2\gamma_1 \tilde{d}_1)) \right\}$$

$$\begin{split} &\cdot \left[\frac{1}{8\gamma_1^2}\sinh(\gamma_1\tilde{d}_1) + \frac{1}{4\gamma_1}\tilde{d}_1\cosh(\gamma_1\tilde{d}_1)\right] + \frac{1}{4}\tilde{d}_1^2\sinh(\gamma_1\tilde{d}_1)\right\},\\ \psi_{12}(0) &= \frac{1}{\gamma_1\tilde{d}_1}\bigg\{\frac{1}{4\gamma_1}\sinh(\gamma_1\tilde{d}_1)\tilde{d}_1\cosh(2\gamma_1\tilde{d}_1) - \sinh(2\gamma_1\tilde{d}_1)\\ &\cdot \left[\frac{1}{8\gamma_1^2}\sinh(\gamma_1\tilde{d}_1) + \frac{1}{4\gamma_1}\tilde{d}_1\cosh(\gamma_1\tilde{d}_1)\right] + \frac{1}{2}\tilde{d}_1^2\cosh(\gamma_1\tilde{d}_1)\bigg\},\\ \psi_{22}(\tilde{d}) &= \frac{\rho_r c_r}{\gamma_1k_r^2\tilde{d}_1}\bigg\{\frac{1}{4\gamma_1}\sinh(\gamma_1\tilde{d}_1)\tilde{d}_1\cosh(2\gamma_1\tilde{d}_1) - \sinh(2\gamma_1\tilde{d}_1)\\ &\cdot \left[\frac{1}{8\gamma_1^2}\sinh(\gamma_1\tilde{d}_1) + \frac{1}{4\gamma_1}\tilde{d}_1\cosh(\gamma_1\tilde{d}_1)\right] + \frac{1}{2}\tilde{d}_1^2\cosh(\gamma_1\tilde{d}_1)\bigg\}. \end{split}$$

For the special case of $\tilde{d}_1 = \tilde{d}_2$, the principle of exchange of stability (PES) for the eigenvalue problems (3.1)-(3.2) can be roughly proved.

Theorem 3.1 (Principle of exchange of stability). Assume that the first eigenvalue $\beta_1(Ma) \in R$. There exists a critical value Ma_c and a neighborhood U of Ma_c such that there exists an unique m with the property

$$\beta_{i}(Ma) \begin{cases} <0, & Ma < Ma_{c}, \\ =0, & Ma = Ma_{c}, \ 1 \le i \le m, \\ >0, & Ma > Ma_{c}, \end{cases}$$
 (3.30)

$$Re\beta_j(Ma_c) < 0, \ j \ge m+1.$$
 (3.31)

for $Ma \in U$

Proof 3.1. Denoting $\psi_1 = (\mathbf{u}_1^c, T_1^c, \mathbf{u}_2^c, T_2^c)$ as the vector corresponding to the eigenvalue $\beta_i(Ma_c)(i=1,\ldots m)$ and using (3.6), one can deduce that

$$\frac{d\beta}{dMa}(Ma_c) = \frac{1}{A} \langle \frac{d}{dMa} L_{Ma_c} \psi, \psi \rangle = \frac{1}{A} Pr \int_{y=0} \frac{\partial T_1^c}{\partial x} u_1^c ds, \qquad (3.32)$$

where

$$A = ||\mathbf{u}_{1}^{c}||_{L^{2}(\Omega_{1})}^{2} + ||T_{1}^{c}||_{L^{2}(\Omega_{1})}^{2} + \rho_{r}||\mathbf{u}_{2}^{c}||_{L^{2}(\Omega_{2})}^{2} + \rho_{r}c_{r}||T_{2}^{c}||_{L^{2}(\Omega_{2})}^{2} > 0.$$

With the help of (3.3) and setting $\beta = 0$, one obtain

$$0 = -Pr||\nabla \mathbf{u}_{1}^{c}||_{L^{2}(\Omega_{1})}^{2} - \rho_{r}||\nabla \mathbf{u}_{2}^{c}||_{L^{2}(\Omega_{2})}^{2} + PrMa_{c} \int_{u=0}^{\infty} \frac{\partial T_{1}^{c}}{\partial x} u_{1}^{c} ds.$$
 (3.33)

Consequently, combing (3.32) and (3.33), one can obtain

$$\frac{d\beta}{dMa}(Ma_c) > 0 \Leftrightarrow \int_{y=0} \frac{\partial T_1^c}{\partial x} u_1^c ds > 0$$
$$\Leftrightarrow Pr||\nabla \mathbf{u}_1^c||_{L^2(\Omega_1)}^2 + \rho_r ||\nabla \mathbf{u}_2^c||_{L^2(\Omega_2)}^2 > 0.$$

Finally, from (3.7), we get (3.31) is valid.

For the generic case $\tilde{d}_1 \neq \tilde{d}_2$, using the same method, one can also obtain the critical value and verify the PES condition.

3.2. Numerical solution of eigenvalue problem

In this subsection, we numerically estimate the critical values of Marangoni number, which not only allow us to demonstrate the validity of the PES condition, but also can be used to calculate transition number.

$ ho_r$	Exact Ma_c (3.29)	Numerical Ma_c	Error
0.644	11782.41122	11782.41262	1.1867×10^{-7}
0.664	5663.23635	5663.23828	3.4100×10^{-7}
0.684	3727.41159	3727.41239	2.1362×10^{-7}
0.704	2777.87118	2777.87121	1.2346×10^{-8}
0.724	2213.89256	2213.88151	4.9911×10^{-6}
0.744	1840.27071	1840.27070	5.0262×10^{-9}
0.764	1574.54646	1574.54653	4.1779×10^{-8}
0.784	1375.87781	1375.87782	1.0374×10^{-8}
0.804	1221.72630	1221.72649	1.5620×10^{-7}

Table 1: Exact critical Maragoni number and numerical critical Marangoni number

Choosing the parameter $Pr=4.38,\ \mu_r=0.812,\ k_r=0.638,\ c_r=1.02,$ $\tilde{l}=6.5,\ \tilde{d}_1=\frac{1}{2},\ \tilde{d}_2=\frac{1}{2},$ the exact critical values of Marangoni number, their numerical estimates and error for $\rho_r\in[0.644,0.844]$ are shown in Table 1. From the Table 1 we can see that the error range is around $10^{-9}\sim10^{-6}$. This means that our numerical method for the eigenvalue problem (3.16)-(3.24) is valid.

Keeping other parameters fixed, we plot the critical values of Marangoni number as a function of height ratio \tilde{d}_1 , aspect ratio \tilde{l} , density ratio ρ_r and heat capacity ratio c_r shown in Figure 3.1 and Figure 3.2. From Figure 3.1 and Figure 3.2, one observes that the critical mode m_c increases with the increasing of the height ratio, aspect ratio, density ratio, but the heat capacity ratio has no effect on the critical mode. At the point where the critical mode changes, two real eigenvalues become critical, which are isolated degenerate cases and beyond the scope of this article. From Figure 3.1, one also observe that the critical values increases as the height ratio increases, which means larger height ratio stablizes the basic state (2.9). Figure 3.2 shows that the critical values decreases with increasing density ratio (heat capacity ratio), meaning that large density ratio (heat capacity ratio) destablizes the basic state (2.9).

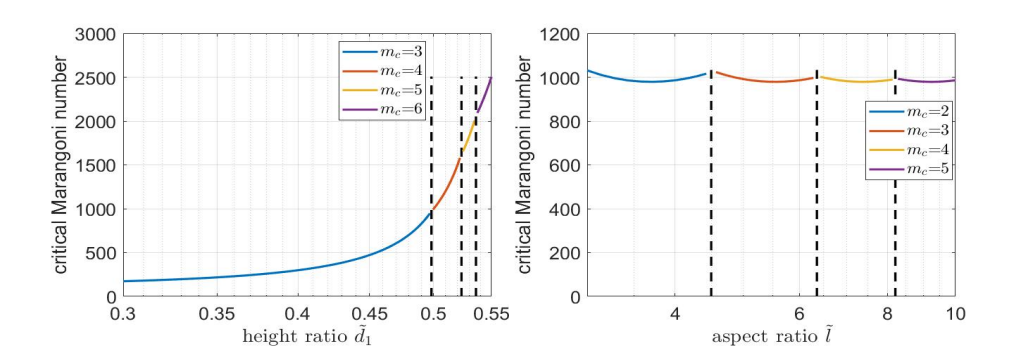


Figure 3.1: Plot of critical value of Marangoni number as a function of $\tilde{d}_1(\text{left})$ and \tilde{l} (right), respectively, where Pr=4.38, $\rho_r=0.844$, $\mu_r=0.812$, $k_r=0.638$, $c_r=1.02$, $\tilde{l}=6.5$ for the left panel, $\tilde{d}_2=\tilde{d}_2=\frac{1}{2}$, for the right panel

.

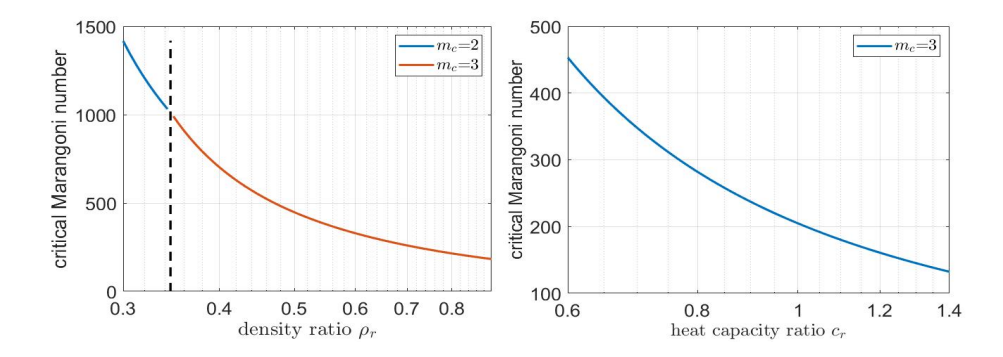


Figure 3.2: Plot of critical values of Marangoni number as a function of ρ_r and c_r , respectively, where $Pr=4.38,\ k_r=0.638,\ \mu_r=0.812,\ \tilde{l}=6.5,\ \tilde{d}_1=\frac{1}{3},\ c_r=1.02$ (left) $\rho_r=0.844$ (right)

.

4. Nonlinear Stability

In this section, we utilize the energy method to analyze the nonlinear stability of (2.12)-(2.24). For the model (2.12)-(2.17), replacing $T_i(i=1,2)$ by $\frac{T_i'}{\sqrt{Ma}}$ and omitting prime, we obtain

$$\frac{\partial \mathbf{u}_1}{\partial t} + (\mathbf{u}_1 \cdot \nabla)\mathbf{u}_1 = -Pr\nabla p_1 + Pr\nabla^2 \mathbf{u}_1, \tag{4.1}$$

$$\frac{\partial T_1}{\partial t} + (\mathbf{u}_1 \cdot \nabla)T_1 = \nabla^2 T_1 + \frac{\sqrt{Ma}}{\tilde{d}_1} v_1, \tag{4.2}$$

$$\operatorname{div}\mathbf{u}_1 = 0, \tag{4.3}$$

and

$$\frac{\partial \mathbf{u}_2}{\partial t} + (\mathbf{u}_2 \cdot \nabla)\mathbf{u}_2 = -\frac{Pr}{\rho_r} \nabla p_2 + \frac{Pr}{\rho_r} \mu_r \nabla^2 \mathbf{u}_2, \tag{4.4}$$

$$\frac{\partial T_2}{\partial t} + (\mathbf{u}_2 \cdot \nabla)T_2 = \frac{k_r}{\rho_r c_r} \nabla^2 T_2 + \frac{\sqrt{Ma}}{k_r \tilde{d}_1} v_2,\tag{4.5}$$

$$\operatorname{div}\mathbf{u}_2 = 0. \tag{4.6}$$

The system of equations (4.1)-(4.6) subject to the same boundary condition (2.23)-(2.22) and the interface condition (2.18),(2.20), but the interface condition (2.19) becomes

$$\mu_r \frac{\partial u_2}{\partial y} - \frac{\partial u_1}{\partial y} + \sqrt{Ma} \frac{\partial T_1}{\partial x} = 0. \tag{4.7}$$

We dot-multiply (4.1), (4.2) with \mathbf{u}_1 and λT_1 , respectively, where $\lambda > 0$ is a free parameter, and Integrate over Ω_1 to obtain

$$\frac{1}{2} \frac{d}{dt} ||\mathbf{u}_1||_{(L^2(\Omega_1))^2}^2 + \int_{\Omega_1} (\mathbf{u}_1 \cdot \nabla) \mathbf{u}_1 \cdot \mathbf{u}_1 dx$$

$$= -Pr||\nabla \mathbf{u}_1||_{(L^2(\Omega_1))^2}^2 + \int_{y=0} Pr \frac{\partial u_1}{\partial y} u_1 ds \tag{4.8}$$

$$\frac{1}{2} \frac{d}{dt} \lambda ||T_1||_{L^2(\Omega_1)}^2 + \lambda \int_{\Omega_1} (\mathbf{u}_1 \cdot \nabla) \mathbf{u}_1 T_1 dx$$

$$= -\lambda ||\nabla T_1||_{L^2(\Omega_1)}^2 + \lambda \frac{\sqrt{Ma}}{\tilde{d}_1} \int_{\Omega_1} v_1 T_1 dx \lambda \int_{y=0} \frac{\partial T_1}{\partial y} T_1 ds. \tag{4.9}$$

Similarly, We dot-multiply (2.15), (2.16) with $\rho_r \mathbf{u}_2$ and $\lambda \rho_r c_r T_1$, respectively, and integrate over Ω_2 to have

$$\frac{1}{2} \frac{d}{dt} \rho_r ||\mathbf{u}_2||_{(L^2(\Omega_2))^2}^2 + \rho_r \int_{\Omega_1} (\mathbf{u}_2 \cdot \nabla) \mathbf{u}_2 \cdot \mathbf{u}_2 dx$$

$$= -Pr\mu_r ||\nabla \mathbf{u}_2||_{(L^2(\Omega_2))^2}^2 - \int_{y=0} Pr\mu_r \frac{\partial u_2}{\partial y} u_2 ds \tag{4.10}$$

$$\frac{1}{2} \frac{d}{dt} \lambda \rho_r c_r ||T_2||^2_{L^2(\Omega_2)} + \lambda \rho_r c_r \int_{\Omega_2} (\mathbf{u}_2 \cdot \nabla) \mathbf{u}_2 T_2 dx$$

$$= -\lambda k_r ||\nabla T_2||^2_{L^2(\Omega_2)} + \lambda \sqrt{Ma} \frac{\rho_r c_r}{k_r \tilde{d}_1} \int_{\Omega_2} v_2 T_2 dx - \lambda k_r \int_{u=0} \frac{\partial T_2}{\partial y} T_2 ds. \quad (4.11)$$

A simple calculation can show that

$$\int_{\Omega_1} (\mathbf{u}_1 \cdot \nabla) \mathbf{u}_1 \cdot \mathbf{u}_1 dx = \int_{\Omega_1} (\mathbf{u}_1 \cdot \nabla) T_1 T_1 dx = 0, \tag{4.12}$$

$$\int_{\Omega_2} (\mathbf{u}_2 \cdot \nabla) \mathbf{u}_2 \cdot \mathbf{u}_2 dx = \int_{\Omega_2} (\mathbf{u}_2 \cdot \nabla) T_2 T_2 dx = 0.$$
 (4.13)

Therefore, making use of (4.12)-(4.13) and adding the equations (4.8)-(4.11) together, we derive that

$$\begin{split} &\frac{1}{2}\frac{d}{dt}[||\mathbf{u}_{1}||_{(L^{2}(\Omega_{1}))^{2}}^{2}+\lambda||T_{1}||_{L^{2}(\Omega_{1})}^{2}+\rho_{r}||\mathbf{u}_{2}||_{(L^{2}(\Omega_{2}))^{2}}^{2}+\lambda\rho_{r}c_{r}||T_{2}||_{L^{2}(\Omega_{2})}^{2}]\\ &=-[Pr||\nabla\mathbf{u}_{1}||_{(L^{2}(\Omega_{1}))^{2}}^{2}+\lambda||\nabla T_{1}||_{L^{2}(\Omega_{1})}^{2}+Pr\mu_{r}||\nabla\mathbf{u}_{2}||_{(L^{2}(\Omega_{2}))^{2}}^{2}\\ &+\lambda k_{r}||\nabla T_{2}||_{L^{2}(\Omega_{2})}^{2}]+\lambda\frac{\sqrt{Ma}}{\tilde{d}_{1}}\int_{\Omega_{1}}T_{1}v_{1}dx+\lambda\sqrt{Ma}\frac{\rho_{r}c_{r}}{k_{r}\tilde{d}_{1}}\int_{\Omega_{2}}T_{2}v_{2}dx \end{split}$$

$$-\int_{y=0} \left[Pr\mu_r \frac{\partial u_2}{\partial y} u_2 - Pr \frac{\partial u_1}{\partial y} u_1\right] ds - \lambda \int_{y=0} \left[k_r \frac{\partial T_2}{\partial y} T_2 - \frac{\partial T_1}{\partial y} T_1\right] ds. \quad (4.14)$$

Making using of the interface conditions (2.18)-(2.20) and (4.7), we obtain

$$\int_{y=0} \left[Pr\mu_r \frac{\partial u_2}{\partial y} u_2 - Pr \frac{\partial u_1}{\partial y} u_1 \right] ds = \int_{y=0} \left[Pr\mu_r u_1 \frac{\partial u_2}{\partial y} - Pru_1 \frac{\partial u_1}{\partial y} \right] ds$$

$$= -Pr\sqrt{Ma} \int_{y=0} \frac{\partial T_1}{\partial x} u_1 ds = -Pr\sqrt{Ma} \int_{y=0} \frac{\partial v_1}{\partial y} T_1 ds$$

$$= -Pr\sqrt{Ma} \int_{\partial \Omega_1} T_1 \frac{\partial \mathbf{u}_1}{\partial y} \cdot \mathbf{n}_1 ds = -Pr\sqrt{Ma} \int_{\Omega_1} \nabla T_1 \cdot \frac{\partial \mathbf{u}_1}{\partial y} dx \qquad (4.15)$$

and

$$\int_{y=0} \left[k_r \frac{\partial T_2}{\partial y} T_2 - \frac{\partial T_1}{\partial y} T_1 \right] ds = \int_{y=0} \left[k_r \frac{\partial T_2}{\partial y} - \frac{\partial T_1}{\partial y} \right] T_1 ds = 0. \tag{4.16}$$

Substituting (4.15)-(4.16) into (4.14), we get

$$\frac{1}{2} \frac{d}{dt} [||\mathbf{u}_{1}||_{(L^{2}(\Omega_{1}))^{2}}^{2} + \lambda ||T_{1}||_{L^{2}(\Omega_{1})}^{2} + \rho_{r} ||\mathbf{u}_{2}||_{(L^{2}(\Omega_{2}))^{2}}^{2} + \lambda \rho_{r} c_{r} ||T_{2}||_{L^{2}(\Omega_{2})}^{2}]$$

$$= -[Pr||\nabla \mathbf{u}_{1}||_{(L^{2}(\Omega_{1}))^{2}}^{2} + \lambda ||\nabla T_{1}||_{L^{2}(\Omega_{1})}^{2} + Pr\mu_{r} ||\nabla \mathbf{u}_{2}||_{(L^{2}(\Omega_{2}))^{2}}^{2}$$

$$+ \lambda k_{r} ||\nabla T_{2}||_{L^{2}(\Omega_{2})}^{2}] + \sqrt{Ma} \left[\lambda \frac{1}{\tilde{d}_{1}} \int_{\Omega_{1}} T_{1} v_{1} dx + \lambda \frac{\rho_{r} c_{r}}{k_{r} \tilde{d}_{1}} \int_{\Omega_{2}} T_{2} v_{2} dx$$

$$+ Pr \int_{\Omega_{1}} \nabla T_{1} \cdot \frac{\partial \mathbf{u}_{1}}{\partial y} dx\right]. \tag{4.17}$$

Let us denote

$$E(t) = \frac{1}{2} [||\mathbf{u}_{1}||_{(L^{2}(\Omega_{1}))^{2}}^{2} + \lambda ||T_{1}||_{L^{2}(\Omega_{1})}^{2} + \rho_{r}||\mathbf{u}_{2}||_{(L^{2}(\Omega_{2}))^{2}}^{2} + \lambda \rho_{r} c_{r}||T_{2}||_{L^{2}(\Omega_{2})}^{2}],$$

$$D = [Pr||\nabla \mathbf{u}_{1}||_{(L^{2}(\Omega_{1}))^{2}}^{2} + \lambda ||\nabla T_{1}||_{L^{2}(\Omega_{1})}^{2} + Pr\mu_{r}||\nabla \mathbf{u}_{2}||_{(L^{2}(\Omega_{2}))^{2}}^{2} + \lambda k_{r}||\nabla T_{2}||_{L^{2}(\Omega_{2})}^{2}],$$

$$I = \lambda \frac{1}{\tilde{d}_{1}} \int_{\Omega_{1}} T_{1} v_{1} dx + \lambda \frac{\rho_{r} c_{r}}{k_{r} \tilde{d}_{1}} \int_{\Omega_{2}} T_{2} v_{2} dx + Pr \int_{\Omega_{1}} \nabla T_{1} \cdot \frac{\partial \mathbf{u}_{1}}{\partial y} dx.$$

$$(4.18)$$

According to (4.18), (4.14) can be rewritten as

$$\frac{dE}{dt} = -D + \sqrt{Ma}I = -D\sqrt{Ma}\left(\frac{1}{\sqrt{Ma}} - \frac{I}{D}\right),\tag{4.19}$$

We define $\frac{1}{\sqrt{Ma_{\lambda}}}$ as the maximum of the ratio of energies

$$\frac{1}{\sqrt{Ma_{\lambda}}} = \max_{H - \{0\}} \frac{I}{D},\tag{4.20}$$

which implies that

$$\frac{dE}{dt} \le -D\sqrt{Ma} \left(\frac{1}{\sqrt{Ma}} - \frac{1}{\sqrt{Ma_{\lambda}}} \right). \tag{4.21}$$

The Poincaré inequality indicates $D \ge cE$ for some constant c. As a result, we deduce from (4.21) that

$$\frac{dE}{dt} \le -c \left(\frac{1}{\sqrt{Ma}} - \frac{1}{\sqrt{Ma_{\lambda}}} \right) E. \tag{4.22}$$

Then, if $\sqrt{Ma} < \sqrt{Ma_{\lambda}}$, the Gronwall lemma indicates that

$$E \le e^{-\tilde{c}t} E(0), \tag{4.23}$$

which yields that the system is nonlinearly stable as long as $\sqrt{Ma} < \sqrt{Ma_{\lambda}}$, where $\tilde{c} = c(\frac{1}{\sqrt{Ma}} - \frac{1}{\sqrt{Ma_{\lambda}}})$.

Next, we shall solve the maximum (4.20), the Euler-Lagrange equations for which read

$$2Pr\nabla^{2}\mathbf{u}_{1} + \lambda \frac{\sqrt{Ma_{\lambda}}}{\tilde{d}_{1}}T_{1}\mathbf{j} - Pr\sqrt{Ma_{\lambda}}\nabla(\frac{\partial T_{1}}{\partial y}) = \nabla L_{1},$$

$$\nabla \cdot \mathbf{u}_{1} = 0, \ (x,y) \in (0,\tilde{l}) \times (-\tilde{d}_{1},0),$$

$$2\nabla^{2}T_{1} + \frac{\sqrt{Ma_{\lambda}}}{\tilde{d}_{1}}v_{1} = 0,$$

$$(4.24)$$

and

$$2Pr\mu_r \nabla^2 \mathbf{u}_2 + \lambda \sqrt{Ma_\lambda} \frac{\rho_r c_r}{k_r \tilde{d}_1} T_2 \mathbf{j} = \nabla L_2,$$

$$\nabla \cdot \mathbf{u}_2 = 0, \ (x, y) \in (0, \tilde{l}) \times (0, \tilde{d}_2),$$

$$2k_r \nabla^2 T_2 + \sqrt{Ma_\lambda} \frac{\rho_r c_r}{k_r \tilde{d}_1} v_2 = 0,$$

$$(4.25)$$

where L_i is the Lagrange multiplier for the region Ω_i (i = 1, 2).

Inserting (3.14)-(3.15) into (4.24)-(4.25) and replacing the p_i by L_i and removing L_i (i = 1, 2), we derive

$$2Pr(D^2 - \gamma_1^2)^2 \varphi_1 - \lambda \frac{\sqrt{Ma_\lambda}}{\tilde{d}_1} \gamma_1^2 \theta_1 = 0,$$

$$2(D^2 - \gamma_1^2)\theta_1 + \frac{\sqrt{Ma_\lambda}}{\tilde{d}_1} \varphi_1 = 0,$$
(4.26)

and

$$2Pr\mu_{r}(D^{2} - \gamma_{1})^{2}\varphi_{2} - \lambda\sqrt{Ma_{\lambda}}\frac{\rho_{r}c_{r}}{k_{r}\tilde{d}_{1}}\gamma_{1}^{2}\theta_{2} = 0,$$

$$2k_{r}(D^{2} - \gamma_{1}^{2})\theta_{2} + \sqrt{Ma_{\lambda}}\frac{\rho_{r}c_{r}}{k_{r}\tilde{d}_{1}}\varphi_{2} = 0,$$
(4.27)

where $D = \frac{d}{dy}$ and $\gamma_1^2 = (\frac{2k_1\pi}{l})^2$. Then, the critical linear eigenvalue problem of (4.1)-(4.6) reads

$$Pr(D^2 - \gamma_1^2)^2 \varphi_1 = 0, (4.28)$$

$$(D^{2} - \gamma_{1}^{2})\theta_{1} + \frac{\sqrt{Ma_{c}}}{\tilde{d}_{1}}\varphi_{1} = 0, \quad y \in (-\tilde{d}_{1}, 0), \tag{4.29}$$

and

$$\mu_r Pr \rho_r^{-1} (D^2 - \gamma_1^2)^2 \varphi_2 = 0, \tag{4.30}$$

$$kr\rho_r^{-1}c_r^{-1}(D^2 - \gamma_1^2)\theta_2 + \frac{\sqrt{Ma_c}}{\tilde{d}_1k_r}\varphi_2 = 0, \quad y \in (0, \tilde{d}_2).$$
 (4.31)

Correspondingly, the condition (4.7) comes

$$\mu_r D^2 \varphi_2(0) - D^2 \varphi_1(0) + \gamma_1^2 \sqrt{M a_\lambda} \theta_1(0) = 0.$$
 (4.32)

The equations (4.26)-(4.27) along with these conditions (3.20), (3.22)-(3.24) and (4.32) constitute a generalized eigenvalue problem for the parameter $\sqrt{Ma_{\lambda}}$. For each $\lambda > 0$, one can solve $\sqrt{Ma_{\lambda}}$ by using the Chebyshev-tau method. By maximizing $\sqrt{Ma_{\lambda}}$ over $\lambda > 0$, we obtain the threshold for nonlinear stability

$$\sqrt{Ma} = \max_{\lambda > 0} \sqrt{Ma_{\lambda}}.$$

The marginal stability curves involving linear and nonlinear stability are shown in Figure 4.1 from which we see that when $\tilde{d}_1 = 0.51$ and $\tilde{d}_1 = 0.54$, the critical value for nonlinear stability is smaller than that for linear stability. This means that the problem (2.12)-(2.24) may undergoes a jump transition.

5. Nonlinear dynamic transitions

5.1. Main result

The Theorem 3.1 says that the system of equations (2.12)-(2.24) must undergo one of three types transitions. In this section, we shall analyze the types

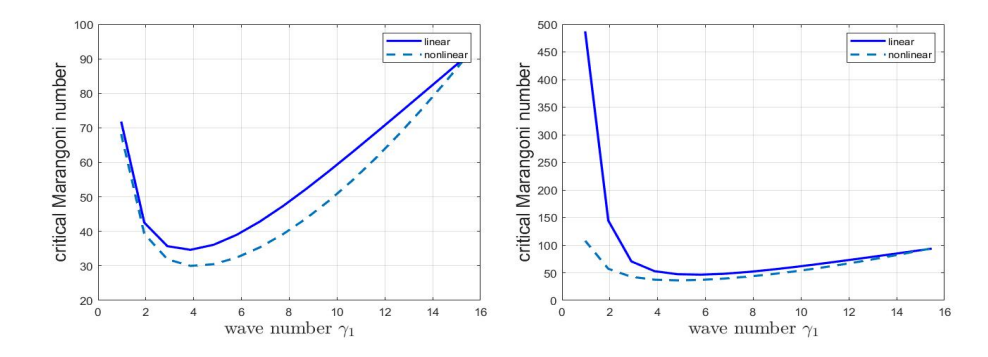


Figure 4.1: Marginal stability curves with $\tilde{d}_1 = 0.51 (\text{left})$ and $\tilde{d}_1 = 0.54$ (right), where $Pr = 4.38, \, \rho_r = 0.844, \, \mu_r = 0.812, \, kr = 0.638, \, \tilde{l} = 6.5.$

.

of transitions when m=2, which is the generic case.

Theorem 5.1. Under the conditions of Theorem 3.1 and assuming m = 2, the exists a coefficient Q defined by (5.16) and depending on the critical values Ma_c and other parameter such that the following assertions hold true

(1) If $Q(Ma_c) < 0$, then the problem (2.12)-(2.24) undergoes a continuous transition from $(0, Ma_c)$. As a result, it bifurcates from $(0, Ma_c)$ to a local attractor \mathcal{A}_{Ma} with the following approximation

$$\mathcal{A}_{Ma} = \left\{ xRe\psi_1 + yIm\psi_1|x^2 + y^2 = -\frac{\beta_1}{Q} \right\} + o\left(\sqrt{\frac{\beta_1}{|Q|}}\right), Ma > Ma_c.$$

The attractor \mathcal{A}_{Ma} is homological to unit circle S^1 , which attracts $H - \Gamma$, where Γ is the stable manifold of $\psi = 0$ with codimension 2.

(2) If $Q(Ma_c) > 0$, then the problem (2.12)-(2.24) undergoes a jump transition from $(0, Ma_c)$. Namely, there exists an open and dense set U of $\psi = 0$ in H such that for any $\psi_0 \in U$ and for every $Ma \in (Ma_c - \epsilon, Ma_c + \epsilon)$ with some $\epsilon > 0$, the solution ψ satisfies

$$\lim_{t \to \infty} \sup ||\psi(t, \psi_0)|| > \sigma_1 > 0,$$

where σ_1 is independent of Ma and Q(Ma).

Proof 5.1. This proof is divided into three parts.

Step1: Space decomposition. According to the spectral theory of linear completely continuous field [55, 50], the spaces V and H can be decomposed into

$$H = E_1 \oplus E_2, \ V = \overline{E_1} \oplus \overline{E_2},$$

where $E_1 = \{\eta_1\psi_1 + \overline{\eta_1}\overline{\psi_1}|\eta_1 \in C\}$, $E_2 = E_1^{\perp}$ and $\psi_1 = (\mathbf{u}_1^c, T_1^c, \mathbf{u}_2^c, T_2^c)$ is the eigenvector corresponding to $\beta_1(Ma_c)$. Therefore, the solution of (2.12)-(2.24) is expressed as

$$\psi = \phi + h(\phi), \ \phi = \eta_1 \psi_1 + \overline{\eta}_1 \overline{\psi}_1 \in E_1, \tag{5.1}$$

where $h: E_1 \to E_2$ is the corresponding center manifold function associated with the PES (3.30) condition. In the vicinity of Ma_c , the center manifold function h can be approximated as

$$h(\phi) = h_2(\phi) + o(|\eta|^2). \tag{5.2}$$

Then, we derive from (2.12)-(2.24) that

$$(\frac{\partial \mathbf{u}_1}{\partial t}, \mathbf{u}_1^*)_1 = -Pr(\nabla \mathbf{u}_1, \nabla \mathbf{u}_1^*)_1 + Pr \int_{u=0}^{u_1} \frac{\partial u_1}{\partial y} u_1^* ds - ((\mathbf{u}_1 \cdot \nabla) \mathbf{u}_1, \mathbf{u}_1^*)_1, \quad (5.3)$$

$$(\frac{\partial T_1}{\partial t}, T_1^*)_1 = -(\nabla T_1, \nabla T_1^*)_1 + \frac{1}{\tilde{d}_1} (v_1, T_1^*)_1 + \int_{y=0} \frac{\partial T_1}{\partial y} T_1^* ds$$
(5.4)

$$-((\mathbf{u}_1\cdot\nabla)T_1,T_1^*)_1,$$

$$(\frac{\partial \mathbf{u}_2}{\partial t}, \mathbf{u}_2^*)_2 = -\frac{Pr\mu_r}{\rho_r} (\nabla \mathbf{u}_2, \nabla \mathbf{u}_2^*)_2 - \frac{Pr\mu_r}{\rho_r} \int_{y=0} \frac{\partial u_2}{\partial y} u_2^* ds - ((\mathbf{u}_2 \cdot \nabla)\mathbf{u}_2, \mathbf{u}_2^*)_2,$$
(5.5)

$$(\frac{\partial T_2}{\partial t}, T_2^*)_2 = -\frac{k_r}{\rho_r c_r} (\nabla T_2, \nabla T_2^*)_2 + \frac{1}{kr\tilde{d}_1} (v_2, T_2^*)_2 - \frac{k_r}{\rho_r c_r} \int_{y=0}^{\infty} \frac{\partial T_2}{\partial y} T_2^* ds - ((\mathbf{u}_2 \cdot \nabla) T_2, T_2^*)_2,$$
(5.6)

where $\psi_1^* = (\mathbf{u}_1^*, T_1^*, \mathbf{u}_2^*, T_2^*)$ is the eigenvector of L_{λ}^* corresponding to β_1 .

For convenience, we denote

$$h_2(\phi) = (h_2^1(\phi), h_2^2(\phi), h_2^3(\phi), h_2^4(\phi)).$$

Multiplying (5.5), (5.6) by ρ_r and $\rho_r c_r$, respectively, then adding these results together with (5.3) and (5.4), one deduce that

$$\begin{split} &\frac{d\eta_{1}}{dt}[(\mathbf{u}_{1}^{c},\mathbf{u}_{1}^{*})_{1}+(T_{1}^{c},T_{1}^{*})_{1}+\rho_{r}(\mathbf{u}_{2}^{c},\mathbf{u}_{2}^{*})_{2}+\rho_{r}c_{r}(T_{2}^{c},T_{2}^{*})_{2}]\\ &=[-Pr(\nabla\mathbf{u}_{1}^{c},\nabla\mathbf{u}_{1}^{*})_{1}-(\nabla T_{1}^{c},\nabla T_{1}^{*})_{1}-\mu_{r}Pr(\nabla\mathbf{u}_{2}^{c},\nabla\mathbf{u}_{2}^{*})_{2}-kr(\nabla T_{2}^{c},\nabla T_{2}^{*})_{2}\\ &+\frac{1}{\tilde{d}_{1}}(T_{1}^{c},v_{1}^{*})_{1}+\frac{\rho_{r}c_{r}}{kr\tilde{d}_{1}}(T_{2}^{c},v_{2}^{*})_{2}+MaPr\int_{y=0}\frac{\partial T_{1}^{c}}{\partial x}u_{1}^{*}]\eta_{1}\\ &-\eta_{1}[((\mathbf{u}_{1}^{c}\cdot\nabla)h_{2}^{1}(\phi)+(h_{2}^{1}(\phi)\cdot\nabla)\mathbf{u}_{1}^{c},\mathbf{u}_{1}^{*})_{1}+((h_{2}^{1}(\phi)\cdot\nabla)T_{1}^{c}\\ &+(\mathbf{u}_{1}^{c}\cdot\nabla)h_{2}^{2}(\phi),T_{1}^{*})_{1}+\rho_{r}((\mathbf{u}_{2}^{c}\cdot\nabla)h_{2}^{3}(\phi)+(h_{2}^{3}(\phi)\cdot\nabla)\mathbf{u}_{2}^{c},\mathbf{u}_{2}^{*})_{2}\\ &+\rho_{c}c_{r}((h_{2}^{3}(\phi)\cdot\nabla)T_{2}^{c}+(\mathbf{u}_{2}^{c}\cdot\nabla)h_{2}^{4}(\phi),T_{2}^{*})_{2}]-\overline{\eta_{1}}[((\overline{\mathbf{u}_{1}^{c}}\cdot\nabla)h_{2}^{1}(\phi)\\ &+(h_{2}^{1}(\phi)\cdot\nabla)\overline{\mathbf{u}_{1}^{c}},\mathbf{u}_{1}^{*})_{1}+((\overline{\mathbf{u}_{1}^{c}}\cdot\nabla)h_{2}^{2}(\phi)+(h_{2}^{1}(\phi)\cdot\nabla)\overline{T_{1}^{c}},T_{1}^{*})_{1}\\ &+\rho_{r}((\overline{\mathbf{u}_{2}^{c}}\cdot\nabla)h_{2}^{3}(\phi)+(h_{2}^{3}(\phi)\cdot\nabla)\overline{\mathbf{u}_{2}^{c}},\mathbf{u}_{2}^{*})_{2}+\rho_{r}c_{r}((\overline{\mathbf{u}_{2}^{c}}\cdot\nabla)h_{2}^{4}(\phi)\\ &+(h_{2}^{3}(\phi)\cdot\nabla)\overline{T_{2}^{c}},T_{2}^{*})_{2}]+o(|\eta_{1}|^{3}). \end{split}$$

With the help of (3.3), one can obtain

$$\frac{d\eta_1}{dt} = \beta_1 \eta_1 + \frac{R(\eta)}{A} + o(|\eta_1|^3), \tag{5.7}$$

where

$$\begin{split} A &= (\mathbf{u}_{1}^{c}, \mathbf{u}_{1}^{*})_{1} + (T_{1}^{c}, T_{1}^{*})_{1} + \rho_{r}(\mathbf{u}_{2}^{c}, \mathbf{u}_{2}^{*})_{2} + \rho_{r}c_{r}(T_{2}^{c}, T_{2}^{*})_{2}, \\ R(\eta) &= -\eta_{1}[((\mathbf{u}_{1}^{c} \cdot \nabla)h_{2}^{1}(\phi) + (h_{2}^{1}(\phi) \cdot \nabla)\mathbf{u}_{1}^{c}, \mathbf{u}_{1}^{*})_{1} + ((h_{2}^{1}(\phi) \cdot \nabla)T_{1}^{c} \\ &+ (\mathbf{u}_{1}^{c} \cdot \nabla)h_{2}^{2}(\phi), T_{1}^{*})_{1} + \rho_{r}((\mathbf{u}_{2}^{c} \cdot \nabla)h_{2}^{3}(\phi) + (h_{2}^{3}(\phi) \cdot \nabla)\mathbf{u}_{2}^{c}, \mathbf{u}_{2}^{*})_{2} \\ &+ \rho_{c}c_{r}((h_{2}^{3}(\phi) \cdot \nabla)T_{2}^{c} + (\mathbf{u}_{2}^{c} \cdot \nabla)h_{2}^{4}(\phi), T_{2}^{*})_{2}] - \overline{\eta_{1}}[((\overline{\mathbf{u}_{1}^{c}} \cdot \nabla)h_{2}^{1}(\phi) \\ &+ (h_{2}^{1}(\phi) \cdot \nabla)\overline{\mathbf{u}_{1}^{c}}, \mathbf{u}_{1}^{*})_{1} + ((\overline{\mathbf{u}_{1}^{c}} \cdot \nabla)h_{2}^{2}(\phi) + (h_{2}^{1}(\phi) \cdot \nabla)\overline{T_{1}^{c}}, T_{1}^{*})_{1} \\ &+ \rho_{r}((\overline{\mathbf{u}_{2}^{c}} \cdot \nabla)h_{2}^{3}(\phi) + (h_{2}^{3}(\phi) \cdot \nabla)\overline{\mathbf{u}_{2}^{c}}, \mathbf{u}_{2}^{*})_{2} + \rho_{r}c_{r}((\overline{\mathbf{u}_{2}^{c}} \cdot \nabla)h_{2}^{4}(\phi) \\ &+ (h_{2}^{3}(\phi) \cdot \nabla)\overline{T_{2}^{c}}, T_{2}^{*})_{2}]. \end{split}$$

Step 2: Center manifold functions. In the following, we calculate the center manifold function $h_2(\phi)$ by following the method used in [56, 52]. Apparently,

the solution of the system

$$\begin{cases} \frac{d}{dt}M\Psi^1 = L_{Ma}\Psi^1, \\ \Psi^1(0) = \eta_1\psi_1 + \overline{\eta_1}\overline{\psi_1}, \end{cases}$$
 (5.8)

is given by

$$\Psi^{1} = \eta_{1} e^{\beta_{1}(Ma)t} \psi_{1} + \overline{\eta_{1}} e^{\overline{\beta_{1}(Ma)t}} \overline{\psi_{1}}. \tag{5.9}$$

Furthermore, we consider the following system

$$\begin{cases} \frac{d}{dt} M \Psi^2 = L_{Ma} \Psi^2 + G(\Psi^1, \Psi^1), \\ \lim_{t \to -\infty} \Psi^2(t) = 0, \end{cases}$$
 (5.10)

where

$$G(\Psi^{1}, \Psi^{1}) = \eta_{1}^{2} exp(2\beta_{1}(Ma)t)(G_{1}(\psi_{1}, \psi_{1}), G_{2}(\psi_{1}, \psi_{1}))^{T}$$

$$+ |\eta_{1}|^{2} exp(Re\beta_{1}(Ma)t)[(G_{1}(\psi_{1}, \overline{\psi_{1}}), G_{2}(\psi_{1}, \overline{\psi_{1}}))^{T}$$

$$+ (G_{1}(\overline{\psi_{1}}, \psi_{1}), G_{2}(\overline{\psi_{1}}, \psi_{1}))^{T}]$$

$$+ \overline{\eta_{1}}^{2} exp(2\overline{\beta_{1}(Ma)}t)(G_{1}(\overline{\psi_{1}}, \overline{\psi_{1}}), G_{2}(\overline{\psi_{1}}, \overline{\psi_{1}}))^{T},$$

and

$$\frac{G_1(\psi_1, \psi_1)}{\exp(2i\gamma_1 x)} = P \begin{pmatrix} i\gamma_1\phi_1^2 + \varphi_1 D\phi_1 \\ i\gamma_1\phi_1\varphi_1 + \varphi_1 D\varphi_1 \\ i\gamma_1\phi_1\theta_1 + \varphi_1 D\theta_1 \end{pmatrix}$$

$$\frac{G_2(\psi_1, \psi_1)}{\exp(2i\gamma_1 x)} = P \begin{pmatrix} \rho_r(i\gamma_1\phi_2^2 + \varphi_2 D\phi_2) \\ \rho_r(i\gamma_1\phi_2\varphi_2 + \varphi_2 D\varphi_2) \\ \rho_r c_r(i\gamma_1\phi_1\theta_1 + \varphi_1 D\theta_1) \end{pmatrix},$$

$$G_1(\psi_1, \overline{\psi_1}) = P \begin{pmatrix} -i\gamma_1|\phi_1|^2 + \varphi_1 D\overline{\phi_1} \\ -i\gamma_1\phi_1\overline{\phi_1} + \varphi_1 D\overline{\phi_1} \\ -i\gamma_1\phi_1\overline{\theta_1} + \varphi_1 D\overline{\theta_1} \end{pmatrix},$$

$$G_{2}(\psi_{1}, \overline{\psi_{1}}) = P \begin{pmatrix} \rho_{r}(-i\gamma_{1}|\phi_{2}|^{2} + \varphi_{2}D\overline{\phi_{2}}) \\ \rho_{r}(-i\gamma_{1}\phi_{2}\overline{\varphi_{2}} + \varphi_{2}D\overline{\varphi_{2}}) \\ \rho_{r}c_{r}(-i\gamma_{1}\phi_{2}\overline{\theta_{2}} + \varphi_{2}D\overline{\theta_{2}}) \end{pmatrix},$$

$$G_{1}(\overline{\psi_{1}}, \psi_{1}) = \overline{G_{1}(\psi_{1}, \overline{\psi_{1}})} \quad G_{2}(\overline{\psi_{1}}, \psi_{1}) = \overline{G_{2}(\psi_{1}, \overline{\psi_{1}})},$$

$$G_{1}(\overline{\psi_{1}}, \overline{\psi_{1}}) = \overline{G_{1}(\psi_{1}, \psi_{1})} \quad G_{2}(\overline{\psi_{1}}, \overline{\psi_{1}}) = \overline{G_{2}(\psi_{1}, \psi_{1})},$$

from which one can obtain the solution $\Psi^2(t)$ has the following expansion

$$\Psi^{2}(t) = \eta_{1}^{2} \exp(2\beta_{1}(Ma)t + 2i\gamma_{1}x)\tilde{\psi}_{20}(y) + |\eta_{1}|^{2} \exp(2Re\beta_{1}(Ma)t)\tilde{\psi}_{11}(y) + \overline{\eta_{1}}^{2} \exp(2\overline{\beta_{1}(Ma)}t - 2i\gamma_{1}x)\tilde{\psi}_{02}(y),$$
(5.11)

where we denote

$$\begin{split} \tilde{\psi}_{20} &= \{\mathbf{u}_{1,20}(y), T_{1,20}(y), \mathbf{u}_{2,20}(y), T_{2,20}(y)\}, \ \mathbf{u}_{m,20}(y) = (u_{m,20}, v_{m,20}), \\ \tilde{\psi}_{11} &= \{\mathbf{u}_{1,11}(y), T_{1,11}(y), \mathbf{u}_{2,11}(y), T_{2,11}(y)\}, \ \mathbf{u}_{m,11}(y) = (u_{m,11}, v_{m,11}), \ m = 1, 2, \\ \tilde{\psi}_{02} &= \{\mathbf{u}_{1,02}(y), T_{1,02}(y), \mathbf{u}_{2,02}(y), T_{2,02}(y)\}, \ \mathbf{u}_{m,02}(y) = (u_{m,02}, v_{m,02}). \end{split}$$

Substituting (5.11) into (5.10), we deduce that $\tilde{\psi}_{20}$ satisfies the following equations

$$2\beta_1(D^2 - 4\gamma_1^2)v_{1,20} = Pr(D^2 - 4\gamma_1^2)^2v_{1,20} + \mathcal{F}_1,$$

$$2\beta_1 T_{1,20} = (D^2 - 4\gamma_1^2)T_{1,20} + \frac{1}{\tilde{d}_1}v_{1,20} + \mathcal{G}_1, \ y \in (-\tilde{d}_1, 0),$$
(5.12)

and

$$2\beta_1(D^2 - 4\gamma_1^2)v_{2,20} = \frac{Pr}{\rho_r}\mu_r(D^2 - 4\gamma_1^2)^2v_{2,20} + \mathcal{F}_2,$$

$$2\beta_1 T_{2,20} = \frac{k_r}{\rho_r c_r}(D^2 - 4\gamma_1^2)T_{2,20} + \frac{1}{k_r \tilde{d}_1}v_{2,20} + \mathcal{G}_2, \ y \in (0, \tilde{d}_2), \tag{5.13}$$

which subjects to the interface conditions and boundary condition (3.20)-(3.24), and where

$$\mathcal{F}_1 = 2i\gamma_1[D(i\gamma_1\phi_1^2 + \varphi_1 D\phi_1) - 2i\gamma_1(i\gamma_1\phi_1\varphi_1 + \varphi_1 D\varphi_1)]$$

$$\mathcal{G}_1 = -(i\gamma_1\phi_1\theta_1 + \varphi_1D\theta_1),$$

$$\mathcal{F}_2 = 2i\gamma_1[D(i\gamma_1\phi_2^2 + \varphi_2D\phi_2) - 2i\gamma_1(i\gamma_1\phi_2\varphi_2 + \varphi_2D\varphi_2)],$$

$$\mathcal{G}_2 = -(i\gamma_1\phi_2\theta_2 + \varphi_2D\theta_2),$$

Furthermore, with the help of the divergence-free condition and boundary condition, we deduce that

$$v_{m,11}(y) = 0, m = 1, 2,$$

which combining the governing equations implies that

$$u_{m,11}(y) = 0, m = 1, 2.$$

As a result, we deduce that $T_{m,11}(m=1,2)$ are determined by the following equations

$$2Re\beta_1T_{1.11} = D^2T_{1.11} - 2(D\varphi_1\theta_1 + \varphi_1D\theta_1),$$

and

$$2Re\beta_1 T_{2,11} = \frac{k_r}{\rho_r c_r} D^2 T_{2,11} - 2(D\varphi_2 \theta_2 + \varphi_2 D\theta_2),$$

which subjects to the following interface conditions and boundary condition

$$T_{1.11}(0) = T_{2.11}(0), \ k_r D T_{2.11}(0) - D T_{1.11}(0) = 0, \ T_{1.11}(-\tilde{d}_1) = T_{2.11}(\tilde{d}_2) = 0.$$

Finally, using the fact

$$G_m(\overline{\psi_1}, \overline{\psi_1}) = \overline{G_m(\psi_1, \psi_1)}, \ m = 1, 2,$$

 $we\ deduce\ that$

$$\tilde{\psi}_{0,2} = \overline{\tilde{\psi}_{2,0}}.$$

Consequently, the approximation center manifold function is given by

$$h_2(\phi) = \Psi^2(t)|_{t=0} = \eta_1^2 \exp(2i\gamma_1 x)\tilde{\psi}_{20}(y) + |\eta_1|^2 \tilde{\psi}_{11}(y) + \overline{\eta_1}^2 \exp(-2i\gamma_1 x)\tilde{\psi}_{02}(y) + o(|\eta_1|^2).$$
 (5.14)

Step 3: Equations reduction. Next, we shall calculate the coefficient R in the reduced equation (5.7). With the help of (5.14), one can deduce

$$R(\eta_1) = \eta_1 |\eta_1|^2 \sum_{i=1}^7 r_i,$$

where

$$\begin{split} r_1 &= -\tilde{l} \int_{-\bar{d}_1}^0 \varphi_1 D T_{1,11} \overline{\theta_1^*} dy - \rho_r c_r \tilde{l} \int_0^{\bar{d}_2} \varphi_2 D T_{2,11} \overline{\theta_2^*} dy \\ r_2 &= -\frac{\tilde{l}}{\gamma_1^2} \int_{-\bar{d}_1}^0 D \overline{\varphi_1} D v_{1,20} D \overline{\varphi_1^*} dy - \frac{\tilde{l}}{2\gamma_1^2} \int_{-\bar{d}_1}^0 \overline{\varphi_1} D^2 v_{1,20} D \overline{\varphi_1^*} dy \\ &- 2\tilde{l} \int_{-\bar{d}_1}^0 D \overline{\varphi_1} v_{1,20} \overline{\varphi_1^*} dy - \tilde{l} \int_{-\bar{d}_1}^0 \overline{\varphi_1} D v_{1,20} \overline{\varphi_1^*} dy \\ r_3 &= -(-\frac{\tilde{l}}{2\gamma_1^2}) \int_{-\bar{d}_1}^0 D v_{1,20} D \overline{\varphi_1} D \overline{\varphi_1^*} dy - (-\frac{\tilde{l}}{\gamma_1^2}) \int_{-\bar{d}_1}^0 v_{1,20} D^2 \overline{\varphi_1} D \overline{\varphi_1^*} dy \\ &- \frac{\tilde{l}}{2} \int_{-\bar{d}_1}^0 D v_{1,20} \overline{\varphi_1} \overline{\varphi_1^*} dy - \tilde{l} \int_{-\bar{d}_1}^0 v_{1,20} D \overline{\varphi_1} \overline{\varphi_1^*} dy \\ r_4 &= -2\tilde{l} \int_{-\bar{d}_1}^0 D \overline{\varphi_1} T_{1,20} \overline{\theta_1^*} dy - \tilde{l} \int_{-\bar{d}_1}^0 v_{1,20} D \overline{\theta_1} \overline{\theta_1^*} dy \\ &- \frac{\tilde{l}}{2} \int_{-\bar{d}_1}^0 D v_{1,20} \overline{\theta_1} \overline{\theta_1^*} dy - \tilde{l} \int_{-\bar{d}_1}^0 v_{1,20} D \overline{\theta_1} \overline{\theta_1^*} dy \\ r_5 &= -\rho_r [\frac{\tilde{l}}{\gamma_1^2} \int_0^{\bar{d}_2} D \overline{\varphi_2} D v_{2,20} D \overline{\varphi_2^*} dy + \frac{\tilde{l}}{2\gamma_1^2} \int_0^{\bar{d}_2} \overline{\varphi_2} D^2 v_{2,20} D \overline{\varphi_2^*} dy \\ &+ 2\tilde{l} \int_0^{\bar{d}_2} D \overline{\varphi_2} v_{2,20} \overline{\varphi_2^*} dy + \tilde{l} \int_0^{\bar{d}_2} \overline{\varphi_2} D v_{2,20} \overline{\varphi_2^*} dy] \\ r_6 &= -\rho_r [(-\frac{\tilde{l}}{2\gamma_1^2}) \int_0^{\bar{d}_2} D v_{2,20} D \overline{\varphi_2} D \overline{\varphi_2^*} dy + (-\frac{\tilde{l}}{\gamma_1^2}) \int_0^{\bar{d}_2} v_{2,20} D^2 \overline{\varphi_2^*} dy] \\ r_7 &= -\rho_r c_r [2\tilde{l} \int_0^{\bar{d}_2} D \overline{\varphi_2} T_{2,20} \overline{\theta_2^*} dy + \tilde{l} \int_0^{\bar{d}_2} \overline{\varphi_2} D T_{2,20} \overline{\theta_2^*} dy] \\ &- \rho_r c_r [\frac{\tilde{l}}{2} \int_0^{\bar{d}_2} D v_{2,20} \overline{\theta_2} \overline{\theta_2^*} dy + \tilde{l} \int_0^{\bar{d}_2} \overline{\varphi_2} D T_{2,20} \overline{\theta_2^*} dy]. \end{split}$$

Then the reduce equation (5.7) can be rewritten as

$$\frac{d\eta_1}{dt} = \beta_1 \eta_1 + Q\eta_1 |\eta_1|^2 + o(|\eta_1|^3), \tag{5.15}$$

where

$$Q = \frac{1}{A} \sum_{i=1}^{7} r_i. {(5.16)}$$

Consequently, by Theorem 2.3.1 in [50], one can obtain the assertions.

6. Numerical results

In the preceding section, we establish the nonlinear dynamic transition theorem of (2.12)-(2.24). The transition type of (2.12)-(2.24) is determined by the sign of the transition number Q. For the purpose of illustration, we give some numerical results on the transition number Q. In Figure 6.1, we plot

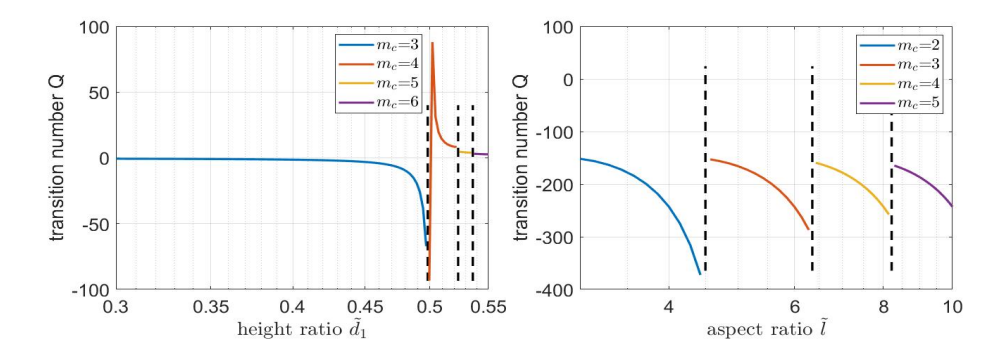


Figure 6.1: Plot of the transition number as a function of \tilde{d}_1 (left) and \tilde{l} (right), respectively. The parameters are: $Pr=4.38,\, \rho_r=0.844,\, \mu_r=0.812,\, k_r=0.638,\, c_r=1.02,\, \tilde{l}=6.5$ for the left panel, $\tilde{d}_1=\frac{1}{2}$ for the right panel

.

the transition number as a function of height ratio \tilde{d}_1 (left) and aspect ratio \tilde{l} (right), respectively. It can be seen from Figure 6.1 that when the value range of height ratio is [0.3, 0.5], the sign of transition number Q is negative. However, when the value range of height ratio is (0.5, 0.55], the sign of transition number Q is positive. By the assertions of Theorem 5.1, the problem (2.12)-(2.24) undergoes a continuous transition for $\tilde{d}_1 \in [0.3, 0.5]$ and a jump transition for $\tilde{d}_1 \in (0.5, 0.55]$. As a result, the problem (2.12)-(2.24) bifurcates a local attractor from $(0, Ma_c)$ for $\tilde{d}_1 \in [0.3, 0.5]$. It is worth pointing out jump transition is

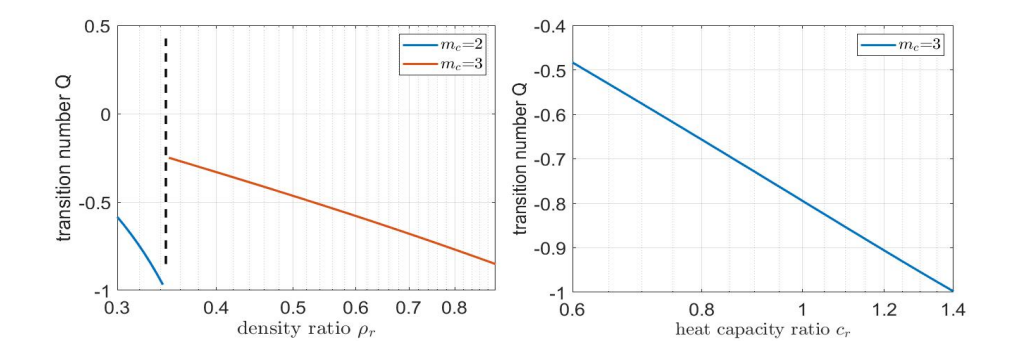


Figure 6.2: Plot of the transition number as a function of ρ_r (left) and c_r (right), respectively. The parameters are: $Pr=4.38,\ k_r=0.638,\ \mu_r=0.812,\ \tilde{l}=6.5,\ \tilde{d}_1=\frac{1}{3},\ c_r=1.02,$ for the left panel, $\rho_r=0.844,$ for the right panel

not observed in the classical Marangoni convection problem in a single domain [28]. Similarly, it can be deduced from Figure 6.1that the problem (2.12)-(2.24) has a continuous transition for $\tilde{l} \in [6, 10]$. In Figure 6.2, we plot the transition number as a function of density ratio ρ_r (left) and heat capacity ratio c_r (right), respectively, it shows that when the density ratio $\rho_r \in [0.3, 0.9]$ or the heat capacity ratio $c_r \in [0.6, 1.4]$, the problem (2.12)-(2.24) will undergo a continuous transition at the critical value $Ma = Ma_c$.

Furthermore, we observe from Figure 6.1 and Figure 6.2 that the transition number Q is discontinuities at those values of height ratio \tilde{d}_1 , aspect ratio \tilde{l}_1 and density ratio ρ_r , where the critical mode m_c changes its value and two eigenvalues become critical eigenvalues. At these points, we cannot apply the reduced equation (5.15) to discuss the transition type of the model (2.12)-(2.24). As mentioned in [52], the change of the critical mode m_c leads to the change of the number of convection rolls. To illustrate this phenomena, we plot the streamline of flow field with height ratios $\tilde{d}_1 = 1/3, 1/2, 0.53, 0.54$, respectively, shown in Figure 6.3-Figure 6.6. From Figure 6.3-Figure 6.6, it is clear that the flow changes from six rolls for $\tilde{d}_1 = 1/3$ and eight rolls for $\tilde{d}_1 = 1/2$ to ten rolls for $\tilde{d}_1 = 0.53$ and twelve rolls for $\tilde{d}_1 = 0.54$, which is consistent with the change

of critical mode m_c shown in Figure 6.1 (lelft). We have similar conclusions from Figure 6.1 (right) and shown in Figure 6.2 (left)

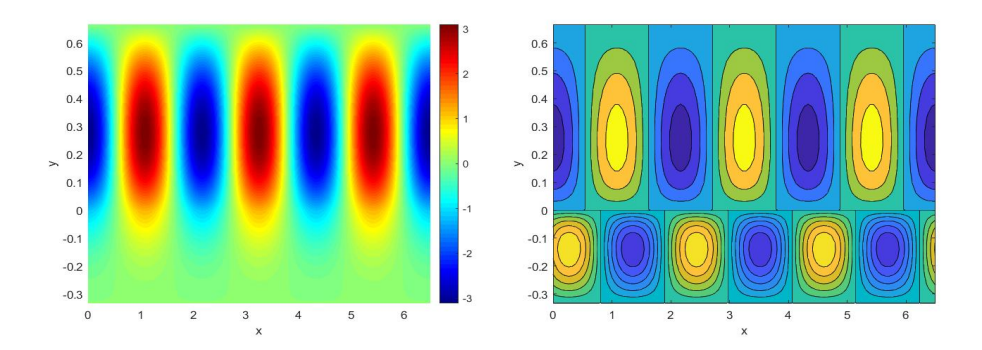


Figure 6.3: The approximate bifurcated solutions-temperature (left), streamline of flow field (right). The parameters are: $Pr=4.38, k_r=0.638, \mu_r=0.812, \rho_r=0.844, \tilde{l}=6.5, \tilde{d}_1=\frac{1}{3}, c_r=1.02$

.

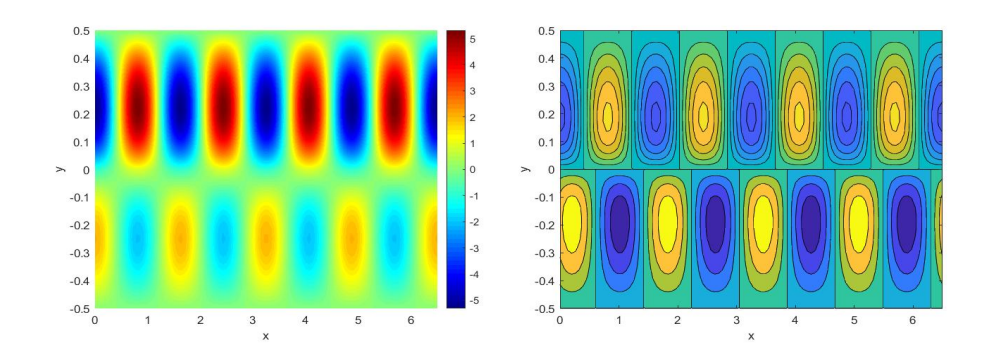


Figure 6.4: The approximate bifurcated solutions-temperature (left), streamline of flow field (right). The parameters are: $Pr=4.38, k_r=0.638, \mu_r=0.812, \rho_r=0.844, \tilde{l}=6.5, \tilde{d}_1=\frac{1}{2}, c_r=1.02$

.

7. Conclusion

In this article, we study nonlinear stability and transition types involving Marangoni convection of two superimposed immiscible fluids with a non-

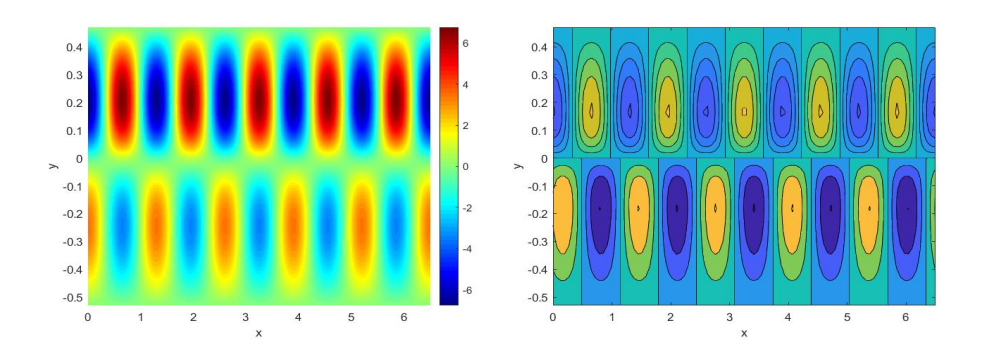


Figure 6.5: The approximate bifurcated solutions-temperature (left), streamline of flow field (right). The parameters are: $Pr=4.38,~k_r=0.638,~\mu_r=0.812,~\rho_r=0.844,~\tilde{l}=6.5,~\tilde{d}_1=0.53,~c_r=1.02$

.

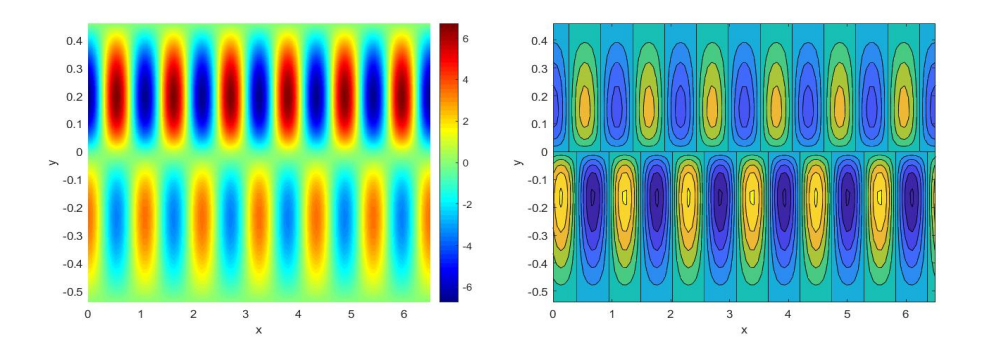


Figure 6.6: The approximate bifurcated solutions-temperature (left), streamline of flow field (right). The parameters are: $Pr=4.38,~k_r=0.638,~\mu_r=0.812,~\rho_r=0.844,~\tilde{l}=6.5,~\tilde{d}_1=0.54,~c_r=1.02$

.

deformable interface by using a hybrid analytical calculation method. Performing careful numerical calculations, we find that the nonlinear stability threshold is less than linear stability threshold, which suggests that a jump transition may exists in the two-layer Marangoni convection. To determine the specific types of nonlinear dynamic transition arising in Marangoni convection of two superimposed immiscible fluids, we establish a transition theorem based on the center manifold reduction. The theorem says that if the sign of a dimensionless coefficient is positive, then a jump transition occurs in the two-layer Marangoni convection. Our numerical calculations show that when the height ratio is between 0.5 and 0.55, the sign of the dimensionless coefficient is positive, which guarantees the existence of a jump transition in two-layer Marangoni convection.

The results in this paper can be extended in serval directions which we shall consider in our future works. First, we only consider the dynamic transition from real eigenvalues. It would be interesting to consider the the dynamic transition from complex eigenvalues. Secondly, we would like to investigate the dynamic transition of two-layer Marangoni convection with deformable interface.

Acknowledgments The work of C.Xing is supported by Scientific Research Foundation of Chengdu University of Information Technology grant No.KYTZ 202186. The work of Q.Wang is supported by the Natural Science Foundation of Sichuan Province (No.2022NSFSC1818) and the National Science Foundation of China (No.11901408). We declare that this work does not have any conflicts of interest

8. Appendix

In this section, we discuss the existence of global weak solution by using the Galerkin method. Firstly, we give the definition of weak solution.

Definition 8.1. We say $\psi = (\mathbf{u_1}, T_1, \mathbf{u_2}, T_2) \in L^2(0, \tau; V) \cap L^{\infty}(0, \tau; H), (0 < \tau < \infty)$ is a weak solution of (2.12)-(2.24), if

$$\frac{d}{dt}(\mathbf{u}_1, \tilde{\mathbf{u}}_1)_1 + \frac{d}{dt}\rho_r(\mathbf{u}_2, \tilde{\mathbf{u}}_2)_2 + ((\mathbf{u}_1 \cdot \nabla)\mathbf{u}_1, \tilde{\mathbf{u}}_1)_1 + Pr(\nabla \mathbf{u}_1, \nabla \tilde{\mathbf{u}}_1)_1$$

$$+ \rho_r((\mathbf{u}_2 \cdot \nabla)\mathbf{u}_2, \tilde{\mathbf{u}}_2)_2 + Pr\mu_r(\nabla \mathbf{u}_2, \nabla \tilde{\mathbf{u}}_2)_2 = PrMa \int_{\mathbf{u}=0} \frac{\partial T_1}{\partial x} \tilde{u}_2 ds, \quad (8.1)$$

and

$$\frac{d}{dt}(T_1, \tilde{T}_1)_1 + \frac{d}{dt}\rho_r c_r(T_2, \tilde{T}_2)_2 + ((\mathbf{u}_1 \cdot \nabla)T_1, \tilde{T}_1)_1 + (\nabla T_1, \nabla \tilde{T}_1)_1
+ \rho_r c_r((\mathbf{u}_2 \cdot \nabla)T_2, \tilde{T}_2)_2 + k_r(\nabla T_2, \nabla \tilde{T}_2)_2 = \frac{1}{\tilde{d}_1}(v_1, \widetilde{T}_1)_1 + \frac{\rho_r c_r}{kr\tilde{d}_1}(v_2, \tilde{T}_2)_2, (8.2)$$

for any $\tilde{\psi} = (\tilde{\mathbf{u}}_1, \tilde{T}_1, \tilde{\mathbf{u}}_2, \tilde{T}_2) \in V$ and satisfies the initial data (2.24).

8.1. Existence and uniqueness of weak solution

To show existence of weak solution, we need a prior estimate of the problem (8.1)-(8.2), which is given as follows.

Lemma 8.1. Suppose that $\psi \in L^2(0,\tau;V) \cap L^{\infty}(0,\tau;H), (0 < \tau < \infty)$ is a weak solution of (2.12)-(2.22), then the following inequalities satisfied

$$\sup_{0 \le t \le \tau} [||\mathbf{u_1}||^2_{(L^2(\Omega_1))^2} + \lambda ||T_1||^2_{L^2(\Omega_1)} + \rho_r ||\mathbf{u_2}||^2_{(L^2(\Omega_2))^2} + \lambda \rho_r c_r ||T_2||^2_{L^2(\Omega_2)}]
\le \exp(M\tau) [||\mathbf{u_{10}}||^2_{(L^2(\Omega_1))^2} + \lambda ||T_{10}||^2_{L^2(\Omega_1)} + \rho_r ||\mathbf{u_{20}}||^2_{(L^2(\Omega_2))^2}
+ \lambda \rho_r c_r ||T_{20}||^2_{L^2(\Omega_2)}]$$
(8.3)

and

$$\int_{0}^{\tau} [Pr||\nabla \mathbf{u_{1}}||_{(L^{2}(\Omega_{1}))^{2}}^{2} + \gamma||\nabla T_{1}||_{L^{2}(\Omega_{1})}^{2} + Pr\mu_{r}||\nabla \mathbf{u_{2}}||_{(L^{2}(\Omega_{2}))^{2}}^{2}
+ \gamma k_{r}||\nabla T_{2}||_{L^{2}(\Omega_{2})}^{2}]dt
\leq (1 + \tau exp(M\tau))[||\mathbf{u_{10}}||_{(L^{2}(\Omega_{1}))^{2}}^{2} + \gamma||T_{10}||_{L^{2}(\Omega_{1})}^{2} + \rho_{r}||\mathbf{u_{20}}||_{(L^{2}(\Omega_{2}))^{2}}^{2}
+ \gamma \rho_{r} c_{r}||T_{20}||_{L^{2}(\Omega_{2})}^{2}],$$
(8.4)

where $\lambda = \max\{1, PrMa^2\}$ and $M = \max\{1, \frac{1}{\tilde{d}_1^2}\lambda, c_r\lambda, \frac{1}{k_r^2\tilde{d}_1^2}\}.$

Making use of the standard Galerkin method and Lemma 8.1, we can prove the existence and uniqueness of weak solution for the model (2.12)-(2.24)

Theorem 8.1. Given $\psi_0 = (\mathbf{u}_{10}, T_{10}, \mathbf{u}_{20}, T_{20}) \in H$, the equations (2.12)-(2.24) possess a unique weak solution $\psi = (\mathbf{u}_1, T_1, \mathbf{u}_2, T_2) \in L^{\infty}(0, \tau; H) \cap L^2(0, \tau; V)$ for any $0 < \tau < \infty$.

8.2. Proof of Lemma 8.1

Choosing $\widetilde{\psi} = \psi$ in (8.1)-(8.2) and from (4.17), we get

$$\frac{1}{2} \frac{d}{dt} [||\mathbf{u_1}||^2_{(L^2(\Omega_1))^2} + \lambda ||T_1||^2_{L^2(\Omega_1)} + \rho_r ||\mathbf{u_2}||^2_{(L^2(\Omega_2))^2} + \lambda \rho_r c_r ||T_2||^2_{L^2(\Omega_2)}]
+ [Pr||\nabla \mathbf{u_1}||^2_{(L^2(\Omega_1))^2} + \lambda ||\nabla T_1||^2_{L^2(\Omega_1)} + Pr\mu_r ||\nabla \mathbf{u_2}||^2_{(L^2(\Omega_2))^2}
+ \lambda k_r ||\nabla T_2||^2_{L^2(\Omega_2)}]
= \frac{1}{\tilde{d_1}} \lambda \int_{\Omega_1} T_1 v_1 dx + \frac{\rho_r c_r}{k_r \tilde{d_1}} \lambda \int_{\Omega_2} T_2 v_2 dx + PrMa \int_{\Omega_1} \nabla T_1 \cdot \frac{\partial \mathbf{u_1}}{\partial y} dx. \quad (8.5)$$

Utilizing the Young's inequality, we obtain

$$\frac{1}{\tilde{d}_{1}}\lambda \int_{\Omega_{1}} T_{1}v_{1}dx + \frac{\rho_{r}c_{r}}{k_{r}\tilde{d}_{1}}\lambda \int_{\Omega_{2}} T_{2}v_{2}dx
\leq \frac{1}{\tilde{d}_{1}}\lambda ||T_{1}||_{L^{2}(\Omega_{1})}||\mathbf{u}_{1}||_{(L^{2}(\Omega_{1}))^{2}} + \frac{\rho_{r}c_{r}}{k_{r}\tilde{d}_{1}}\lambda ||T_{2}||_{L^{2}(\Omega_{2})}||\mathbf{u}_{2}||_{(L^{2}(\Omega_{1}))^{2}}
\leq \frac{\lambda}{2}||T_{1}||_{L^{2}(\Omega_{1})}^{2} + \frac{\lambda}{2\tilde{d}_{1}^{2}}||\mathbf{u}_{1}||_{(L^{2}(\Omega_{1}))^{2}}^{2} + \frac{\lambda\rho_{r}c_{r}}{2}||T_{2}||_{L^{2}(\Omega_{2})}^{2} + \frac{\rho_{r}c_{r}\lambda}{2k_{r}^{2}\tilde{d}_{1}^{2}}||\mathbf{u}_{2}||_{(L^{2}(\Omega_{1}))^{2}}^{2}
\leq \frac{M}{2}[||\mathbf{u}_{1}||_{(L^{2}(\Omega_{1}))^{2}}^{2} + \lambda||T_{1}||_{L^{2}(\Omega_{1})}^{2} + \rho_{r}||\mathbf{u}_{2}||_{(L^{2}(\Omega_{1}))^{2}}^{2} + \lambda\rho_{r}c_{r}||T_{2}||_{L^{2}(\Omega_{2})}^{2}],$$
(8.6)

and

$$PrMa \int_{\Omega_{1}} \frac{\partial \mathbf{u_{1}}}{\partial y} \cdot \nabla T_{1} dx$$

$$\leq \frac{1}{2} Pr ||\nabla \mathbf{u_{1}}||_{(L^{2}(\Omega_{1}))^{2}}^{2} + \frac{1}{2} PrMa^{2} ||\nabla T_{1}||_{L^{2}(\Omega_{1})}^{2}$$

$$\leq \frac{1}{2} Pr ||\nabla \mathbf{u_{1}}||_{(L^{2}(\Omega_{1}))^{2}}^{2} + \frac{1}{2} \lambda ||\nabla T_{1}||_{L^{2}(\Omega_{1})}^{2}.$$
(8.7)

Substituting (8.6)-(8.7) into (8.5), one can get

$$\frac{d}{dt}[||\mathbf{u_1}||_{(L^2(\Omega_1))^2}^2 + \lambda||T_1||_{L^2(\Omega_1)}^2 + \rho_r||\mathbf{u_2}||_{(L^2(\Omega_2))^2}^2 + \lambda \rho_r c_r||T_2||_{L^2(\Omega_2)}^2]
+ [Pr||\nabla \mathbf{u_1}||_{(L^2(\Omega_1))^2}^2 + \lambda||\nabla T_1||_{L^2(\Omega_1)}^2 + Pr\mu_r||\nabla \mathbf{u_2}||_{(L^2(\Omega_2))^2}^2
+ \lambda k_r||\nabla T_2||_{L^2(\Omega_2)}^2]
\leq M[||\mathbf{u_1}||_{(L^2(\Omega_1))^2}^2 + \lambda||T_1||_{L^2(\Omega_1)}^2 + \rho_r||\mathbf{u_2}||_{(L^2(\Omega_2))^2}^2 + \lambda \rho_r c_r||T_2||_{L^2(\Omega_2)}^2].$$
(8.8)

Consequently, (8.3)-(8.4) can be derived by the Gronwall's Lemma.

References

- [1] S. Ostrach, Low-gravity fluid flows, Annu.Rev.Fluid Mech. 14 (1982) 313–345.
- [2] L. Ratke, H. Walter, B. Feuerbacher, Material and Fluid under Low Gravity, Springer-Verlag, Berlin, 1989.
- [3] A. L. Frenkel, D. Halpern, Stokes-flow in stability due to interfacial surfactant, Phys. Fluids 14 (2002) L45–L48.
- [4] D. Halpern, A. L. Frenkel, Destabilization of a creeping flow by interfacial surfactant: linear theory extended to all wavenumbers, J. Fluid Mech. 485 (2003) 191–220.
- [5] T. S. Sammarco, M. A. Burns, Thermocapillary pumping of discrete droplets in microfabricated analysis devices, AIChE J. 45 (1999) 350–366.
- [6] D. E. Kataoka, S. M. Troian, Patterning liquid flow on the microscopic scale, Nature 402 (1999) 794–797.
- [7] A. A.Darhuber, J. M. Davis, S. M. Troian, W. W. Reisner, Thermocapillary actuation of liquid flow on chemically patterned surfaces, Phys. Fluids 15 (2003) 1295–1304.
- [8] J. Dowden, Interaction of the keyhole and weld pool in laser keyhole welding, J. Laser Appl. 14 (2002) 204–209.
- [9] T. Fuhrich, P. Berger, H. Hugel, Marangoni effect in laser deep penetration welding of steel, J. Laser Appl. 13 (2001) 178–186.
- [10] M. Maillard, L. Motte, A. T. Ngo, M. P. Pileni, Rings and hexagons made of nanocrystals: a marangoni effect, J. Phys. Chem. B 104 (2000) 11871–11877.
- [11] V. Truskett, K. J. Stebe, Influence of surfactants on an evaporating drop:fluorescence images and particle deposition patterns, Langmuir 19 (2003) 8271–8279.

- [12] N. Maruyama, T. Koito, J. Nishida, T. Sawadaishi, X. Cieren, K. Ijiro, O. Karthaus, M. Shimomura, Mesoscopic patterns of molecular agregates on solid substrates, Thin Solid Films 327 (1998) 854–856.
- [13] O. Pitois, B. Francois, Crystallization of condensation droplets on a liquid surface, Colloid and Polymer Sci. 277 (1999) 574–578.
- [14] O. Pitois, B. Francois, Formation of ordered micro-porous membranes, Eur. Phys. J. B 8 (1999) 225–231.
- [15] M. Srinivasao, D. Collings, A. Philips, S. Patel, Three-dimensionally ordered array of air bubbles in a polymer film, Science 292 (2001) 79–83.
- [16] J. B. Grotberg, O. E. Jensen, Biofluid mechanics in flexible tubes, Annu. Rev. Fluid Mech. 36 (2004) 121–147.
- [17] D. Zelig, S. Haber, Hydrodynamic cleansing of pulmonary alveoli, SIAM J. Appl. Math. 63 (2002) 195–221.
- [18] E. D. Hondros, M. McLean, K. C. Mills, Marangoni and Interfacial Phenomena in Materials Processing: Originating from Contributions to a Discussion of the Royal Society of Londo, The University Press, Cambridge, 1998.
- [19] A. Nepomnyashchy, I. Simanovskii, J. C. Legros, Interfacial Convection in Multilayer Systems, Springer. New York, 2006.
- [20] S. Rosenblat, G. M. Homsy, S. H. Davis, Non-linear marangoni convectionin bounded layers, part 1. circular cylindrical containers, J. Fluid Mech. 120 (1982) 91–122.
- [21] S. Rosenblat, G. M. Homsy, S. H. Davis, Non-linear marangoni convection in bounded layers, part 2. rectangular cylindrical containers, J. Fluid Mech. 120 (1982) 123–1238.
- [22] L. Shtilman, G. Sivashinsky, Hexagonal structure of large-scale marangoni convections, Physica D 52 (1991) 477–488.

- [23] R. Savino, R. Monti, Oscillatory marangoni convection in cylindrical liquid bridges, Phys. Fluids 9 (1996) 2906–2915.
- [24] A. Bergeon, D. Henry, H. Benhadid, L. S. Tuckerman, Marangoni convection in binary mixtures with soret effect, J. Fluid Mech. 375 (1998) 143–177.
- [25] M. Hamed, J. M. Floryan, Marangoni convection. part 1. a cavity with differentially heated sidewalls, J. Fluid Mech. 405 (2000) 79–110.
- [26] M. Hamed, J. M. Floryan, Marangoni convection. part 2. a cavity subject to point heating, J. Fluid Mech. 405 (2000) 111–129.
- [27] A. M. Mancho, H. Riecke, F. Sain, Instabilities and spatio-temporal chaos of long-wave hexagon patterns in rotating marangoni convection, Chaos 12 (2002) 706–718.
- [28] H. Dijkstra, T. Sengul, S. Wang, Dynamic transitions of surface tension driven convection, Phys. D 247 (2013) 7–17. doi:10.1016/j.physd.2012. 12.008.
- [29] G. Guidoboni, B. Jin, On the nonlinear stability of Marangoni-Bénard problem with free surface in the boussineq approximation, Mathematical Models and Methods in Applied Sciences 15 (2005) 1–22. doi:10.1142/S0218202505003873.
- [30] R. Idris, I. Hashim, Effects of controller and cubic temperature profile on onset of Bénard-Marangoni convection in ferrofluid, Int Commun Heat Mass 37 (2010) 624–628. doi:10.1016/j.icheatmasstransfer.2009.11. 015.
- [31] M. Mahmud, Z. Mustafa, I. Hashim, Effects of control on the onset of Bénard - Marangoni convection in a micropolar fluid, Int Commun Heat Mass 37 (2010) 1335-1339. doi:10.1016/j.icheatmasstransfer.2010. 08.013.

- [32] J. Zhu, W. Shi, L. Feng, Bénard-Marangoni instability in sessile droplet evaporating contact angle mode on heated substrate, Int J Heat Mass Tran 134 (2019) 784–795. doi:10.1016/j.ijheatmasstransfer.2019.01.082.
- [33] J. R. Pearson, On convection cells induced by surface tension, J. Fluid Mech. 4 (1958) 489–500.
- [34] K. A. Smith, On convective instability induced by surface-tension gradients, J. Fluid Mech. 24 (1966) 401–414.
- [35] I. B. Simanovskii, A. A. Nepomnyashchy, Convective Instabilities in Systems with Interface, Gordon and Breach, London, 1993.
- [36] A. A. Nepomnyashchy, I. B. Simanovskii, Influence of thermocapillary effect and interfacial heat release on convective oscillations in a two-layer system, Phys. Fluids 16 (2004) 1127–1139.
- [37] A. Engel, J. Swift, Planform selection in two-layer Bénard Marangoni convection, Phys. Rev. E 62 (2000) 6540-6553. doi:10.1103/PhysRevE. 62.6540.
- [38] D. Mo, D. Ruan, Linear stability analysis of thermocapillary buoyancy convection in an annular two layer system with upper rigid wall subjected to a radial temperature gradient, Microgravity Sci Tec. 31 (2019) 293–304. doi:10.1007/s12217-019-9692-3.
- [39] D. Mo, D. Ruan, Linear-stability analysis of thermocapillary convection in an annular two layer system with free surface subjected to a radial temperature gradient, J Mech Sci Technol 32 (2018) 3437–3444. doi: 10.1007/s12206-018-0647-1.
- [40] S. Madruga, C. Pérez-García, G. Lebon, Convective instabilities in two superposed horizontal liquid layers heated laterally, Phys. Rev. E 68 (2003) 041607. doi:10.1103/PhysRevE.68.041607.

- [41] I. Simanovskii, O. Kabov, Nonlinear convective oscillations in two layer systems with different aspect ratios, Microgravity Sci Tec. 24 (2012) 127– 137. doi:10.1007/s12217-012-9305-x.
- [42] S. J. Tavener, K. A. Cliffe, Two fluid Marangoni Bénard convection with a deformable interface, J. Comput. Phys. 182 (2002) 277–300. doi:10.1006/ jcph.2002.7167.
- [43] T. Lyubimova, Y. Parshakova, The influence of thermocapillary effect on the onset of convection in a two layer system with deformable interface and perfectly conductive boundaries, Int J Heat Mass Tran 129 (2019) 610–617. doi:10.1016/j.ijheatmasstransfer.2018.09.099.
- [44] A. Juel, J. Burgess, W. McCormick, J. Swift, H. Swinney, Surface tension-driven convection patterns in two liquid layers, Phys. D 143 (2000) 169–186. doi:10.1016/S0167-2789(00)00100-7.
- [45] R. Liu, Q. Liu, The convective instabilities in a liquid vapor system with a non-equilibrium evaporation interface, Microgravity Sci Tec. 21 (2009) 233–240. doi:10.1007/s12217-009-9126-8.
- [46] A. Nepomnyashchy, I. Simanovskii, Novel criteria for the development of monotonic and oscillatory instabilities in a two layer film, Phys Fluid 29 (2017) 092104. doi:10.1063/1.5001729.
- [47] A. Nepomnyashchy, I. Simanovskii, Convective flows in a two layer system with a temperature gradient along the interface, Phys Fluid 18 (2006) 032105. doi:10.1063/1.2181807.
- [48] I. Simanovskii, A. Nepomnyashchy, V. Shevtsova, P. Colinet, J. Legros, Nonlinear Marangoni convection with the inclined temperature gradient in multilayers systems, Phys. Rev. E 73 (2006) 066310. doi:10.1103/ PhysRevE.73.066310.

- [49] W. Shi, S. Rong, L. Feng, Marangoni convection instabilities induced by evaporation of liquid layer in an open rectangular pool, Microgravity Sci Tec. 29 (2017) 91–96. doi:10.1007/s12217-016-9528-3.
- [50] T. Ma, S. Wang, Phase transition dynamics, Springer. New York, 2014. doi:10.1007/978-1-4614-8963-4.
- [51] H. Dijkstra, T. Sengul, J. Shen, S. Wang, Dynamic transitions of quasi-geostrophic channel flow, SIAM J. Appl. Math. 75 (2015) 2361–2378. doi: 10.1137/15M1008166.
- [52] D. Han, Q. Wang, X. Wang, Dynamic transitions and bifurcations for thermal convection in the superposed free flow and porous media, Phys. D 414 (2020) 132687, 17. doi:10.1016/j.physd.2020.132687.
- [53] C. Lu, Y. Mao, T. Sengul, Q. Wang, On the spectral instability and bifurcation of 2d-quasi-geostrophic potential vorticity equation with a generalized kolmogorov forcing, Phys. D 403 (2020) 132296, 18. doi: 10.1016/j.physd.2019.132296.
- [54] C. Lu, Y. Mao, Q. Wang, D. Yan, Hopf bifurcation and transition of threedimensional wind-driven ocean circulation problem, J. Differential Equations 267 (2019) 2560–2593. doi:10.1016/j.jde.2019.03.021.
- [55] T. Ma, S. Wang, Bifurcation theory and applications, World Scientific Pub. Co. Inc., 2005. doi:10.1142/5798.
- [56] C. Kieu, T. Sengul, Q. Wang, D. Yan, On the Hopf (double Hopf) bifurcations and transitions of two-layer western boundary currents, Commun. Nonlinear Sci. Numer. Simul. 65 (2018) 196–215. doi:10.1016/j.cnsns. 2018.05.010.